

# Eigenvector-based acceleration strategies for gradient-type methods

Jean-Paul Chehab\*      Gaspard Kemlin†      Marcos Raydan‡      Yousef Saad§

## Abstract

Several strategies are described and analyzed to speed-up gradient-type methods when applied to the minimization of strictly convex quadratics and strictly convex functions. The proposed techniques focus on relaxing the traditional optimal step length associated with gradient methods, including the steepest descent (SD) and the minimal residual (MR) methods. Such a relaxation avoids the well-known negative zigzag effect and allows the iterates to move in the entire space which in turn implies that every so often the search direction approaches some eigenvector of the underlying Hessian matrix. The proposed speedups then rely on taking advantage of the properties of the Lanczos method once a search direction that approaches an eigenvector has been identified in order to accelerate the convergence towards the global minimizer. After analyzing the proposed strategies, we illustrate them on the global minimization of strictly convex functions.

**Keywords:** Gradient-type methods, Lanczos method, convex optimization

**AMS Subject Classification:** 65F10, 65K05, 15A06, 90C25, 90C06

## 1 Introduction

Gradient-type methods are still widely used for solving the following large-scale optimization problem

$$\min_{x \in \mathbb{R}^n} f(x), \quad (1)$$

where  $f : \mathbb{R}^n \rightarrow \mathbb{R}$  is continuously differentiable. From a given initial guess  $x_0 \in \mathbb{R}^n$ , they are described by the following iterative scheme

$$x_{k+1} = x_k - \alpha_k g_k, \quad (2)$$

where  $g_k = \nabla f(x_k)$  is the gradient at  $x_k$ , and  $\alpha_k > 0$  is the steplength determined by the method. Some of the advantages that motivate the current use of gradient-type methods include: they are simple to understand and implement; they require relatively low memory and can handle a large number of variables making them suitable for big data and large-scale machine learning applications, see, e.g., [3, 4, 6]; and they are often supported by strong theoretical convergence results. For instance, under standard conditions, they are guaranteed to converge to a local minimum or even a global minimum in the case of convex functions [2, 5, 14]. However, it is also well known that the most popular gradient-type methods, in which the step length is chosen to be optimal in some sense, may take many iterations to locate a solution as their asymptotic behavior depends on the spectral properties of the Hessian matrix of  $f$ , so they may struggle in the presence of ill-conditioning; see, e.g., [10, 11, 13, 25] and references therein. For the sake of completeness, we briefly recall the two most emblematic gradient-type methods.

\*LAMFA (UMR CNRS 7352), Université de Picardie Jules Verne, France ([jean-paul.chehab@u-picardie.fr](mailto:jean-paul.chehab@u-picardie.fr)).

†LAMFA (UMR CNRS 7352), Université de Picardie Jules Verne, France ([gaspard.kemlin@u-picardie.fr](mailto:gaspard.kemlin@u-picardie.fr)).

‡Center for Mathematics and Applications (NovaMath), FCT NOVA, Portugal ([m.raydan@fct.unl.pt](mailto:m.raydan@fct.unl.pt)).

§Department of Computer Science and Engineering, University of Minnesota, USA ([saad@umn.edu](mailto:saad@umn.edu)).

Cauchy's steepest descent (SD) algorithm [7] is the oldest gradient-type method for solving (1), and its optimal choice of steplength  $\alpha_k^{\text{SD}}$  is given by

$$\alpha_k^{\text{SD}} := \arg \min_{\alpha} f(x_k - \alpha g_k). \quad (3)$$

The poor practical behavior of (2)-(3) has been known for many decades. In the late 1950s, Akaike [1] characterized the asymptotic behavior of the method for strictly convex quadratic functions. Akaike established that, with the choice of steplength (3), the search directions asymptotically alternate within the two-dimensional subspace spanned by the eigenvectors corresponding to the largest and smallest eigenvalues of the constant Hessian matrix of  $f$ . Moreover, in that case,  $g_{k+1}^T g_k = 0$  for all  $k$ . This combination of facts causes SD to zig-zag on a 2-dimensional subspace as it approaches the minimizer, and hence it can be very slow on ill-conditioned problems. We recommend [13] for a deeper understanding of this type of negative behavior of the SD method.

Closely related to SD is the Minimal Gradient method; see, e.g., [8, 9, 15] (which in the case of solving linear systems is better known as the minimal residual (MR) method). In the MR method, the optimal steplength  $\alpha_k^{\text{MR}}$  minimizes the 2-norm of the gradient at the next iterate

$$\alpha_k^{\text{MR}} := \arg \min_{\alpha} \|\nabla f(x_k - \alpha g_k)\|. \quad (4)$$

Many of the asymptotic results for SD carry over analogously to the MR method. It is widely accepted that the MR method, given by (2)-(4), can also perform poorly and has similar asymptotic behavior as the SD method, i.e., it asymptotically zigzags in a two-dimensional subspace; see [15] for a formal proof of these facts.

Consequently, a tempting and perhaps surprising option to avoid the zigzag curse, which in turn produces extremely slow schemes, is to disturb the exact optimal choice of steplength associated with the negative gradient direction. In this regard, Raydan and Svaiter [19] investigate the random choice of a parameter in  $(0, 2)$  that multiplies the optimal step length, to avoid the zigzag effect. They study that random mechanism, precisely to stress out that the poor behavior of the SD method is due to the optimal choice of steplength and not to the choice of the search direction, and indeed a significant improvement on the behavior of the SD method is observed. It is worth noticing that they provide theoretical guarantees, confirming that SD with random relaxation converges to the unique global minimizer when dealing with strictly convex quadratic functions. In the last two decades, several variants and improved relaxation schemes have been proposed and analyzed that also avoid the optimal step length and thus the zigzag curse; see, e.g., [25] for a comprehensive review. Recently, in [18], much insight has been added to the topic of relaxed steplength selection, and the convergence of a large family of options has been studied. We also refer to [16] for a study of the steepest descent algorithm with fully random steplengths.

In this paper, in order to accelerate the gradient-type methods (2), we add understanding to the relaxed techniques for breaking the zigzagging pattern, and also propose and analyze several strategies to speed-up gradient-type methods when applied to the minimization of strictly convex quadratics and strictly convex functions. Once the zigzag curse is avoided, our speed-up schemes take advantage of the relationship between (2) and the shifted power method, which in turn implies that every so often the residual approaches some eigenvector of the underlying Hessian matrix, therefore providing ideal search directions. The most effective proposed speedup scheme in this work then relies on taking advantage of the properties of the Lanczos method once a search direction that approaches an eigenvector has been identified. The idea of exploiting the alignment of the search direction with eigendirections of the Hessian matrix to construct appropriate steplengths have also been explored in different ways in [10, 12]. The main novelty of the present work is then the combination of the relaxed gradient-type methods with the Lanczos algorithm to fully exploit ideal search directions once the gradient approaches some eigenvector of the Hessian matrix. In particular, we show that this allows to reach the sought-after minimizer with a reduced number of matrix-vector products.

The rest of the paper is organized as follows. Section 2 is dedicated to some review of standard results on the MR and SD methods for minimizing quadratic functionals. We also make some numerical observations which are the motivation for the various spectral acceleration techniques from Section 3. The latter is at the heart of the paper: we introduce an acceleration method based on Lanczos subspace iterations, with various adaptive variants, that we complete with an analogy to algebraic multigrid methods. Section 4 is then dedicated to the extension of these accelerations techniques to the global minimization of nonquadratic convex functions. Finally, in Section 5, we analyze mathematically and prove a number of results on the observations made in Section 2.

## 2 Numerical observations for quadratic functionals

**General considerations on quadratic functionals.** An important nonlinear instance of (1) is the minimization of the strictly convex quadratic:

$$f(x) = \frac{1}{2}x^\top Ax - b^\top x, \quad (5)$$

where  $b \in \mathbb{R}^n$  and  $A \in \mathbb{R}^{n \times n}$  is a symmetric and positive definite (SPD) matrix. Since  $A$  is SPD and the gradient  $g(x) \equiv \nabla f(x) = Ax - b$ , then the global minimizer of (5) is the unique solution  $x^* = A^{-1}b$  of the linear system  $Ax = b$ . The solution of (5) is of fundamental importance in the field of applied mathematics and in numerous engineering developments; see [21]. Moreover, solving it efficiently is usually a pre-requisite for a method to be generalized to solve more general optimization problems. In addition, by Taylor's expansion, a general smooth function can be approximated by a quadratic function near a minimizer. Thus, the local convergence behavior of gradient methods is often reflected by solving (5). For this reason, we make in this section, a number of observations that are relevant to motivate the proposed acceleration schemes, introduced in Section 3.

First, for solving (5), the optimal steplengths for SD and MR are respectively given by, with  $g_k = \nabla f(x_k)$ ,

$$\alpha_k^{\text{SD}} = \frac{g_k^\top g_k}{g_k^\top A g_k} \quad (6)$$

$$\alpha_k^{\text{MR}} = \frac{g_k^\top A g_k}{g_k^\top A^2 g_k}. \quad (7)$$

Notice that both steplengths defined above are inverses of Rayleigh quotients of  $A$  for some special vector in  $\mathbb{R}^n$ . By simple algebraic manipulations, if we apply either SD or MR to solve (5) but multiplying by 2 their optimal step lengths, it follows that, for all  $k \in \mathbb{N}$ ,

$$f(x_k - 2\alpha_k^{\text{SD}} g_k) = f(x_k) \quad \text{and} \quad \|\nabla f(x_k - 2\alpha_k^{\text{MR}} g_k)\| = \|\nabla f(x_k)\|.$$

Hence, by continuity and strict convexity of both merit functions, using any fixed relaxation parameter  $\sigma \in (0, 2)$  to multiply the optimal steplength of either SD or MR produces iterative methods for which the functions  $f(x)$  or  $\|\nabla f(x)\|$  are monotonically decreasing. Moreover, for such relaxed gradient-type schemes convergence of the iterates to the unique solution of (5) is guaranteed. Most important, as long as  $\sigma \neq 1$  (except perhaps for a few selected iterations) the zigzag curse in a 2-dimensional subspace is avoided, and the iterates move in the entire  $n$ -dimensional space; see [18, pp. 178-179] and [19] for details. However, in this case, the behavior of the iterations is not easily analyzed as it exhibits a chaotic behavior [22]. What is rather interesting is the speed-up observed for the situation when  $\sigma \neq 1$ . Specifically, as discussed in [22, Section 8], to avoid a possible chaotic behavior it is recommended to choose the factor  $\sigma \in (0, 1)$  which has proved to be more effective. In fact, experiments with relaxation values of  $\sigma \in (1, 2)$  have been reported in [18] to produce a significant slower behavior (in the sense that more iterations are required to achieve convergence), sometimes even worse than using  $\sigma = 1$ ; see also [22, Section 5].

Now we recall that, for a given relaxation parameter  $\sigma \in (0, 2)$ , the relaxed gradient-type method reads

$$x_{k+1} = x_k - \sigma \alpha_k g_k \quad \text{for } \sigma \neq 1, \quad (8)$$

where  $\alpha_k$  stands either for  $\alpha_k^{\text{SD}}$ ,  $\alpha_k^{\text{MR}}$ . Notice that multiplying by  $A$  and subtracting the vector  $b$  on both sides, we obtain the gradient vector at step  $k + 1$ :

$$g_{k+1} = g_k - \sigma \alpha_k A g_k = (I - \sigma \alpha_k A) g_k = \left( \prod_{i=0}^k (I - \sigma \alpha_i A) \right) g_0. \quad (9)$$

This establishes a relationship between the sequence  $(g_k)_{k \in \mathbb{N}}$  generated by (8) and the shifted power method. It is worth noting that this connection with the shifted power method holds in principle for any gradient-type method applied to (5). However, this relationship is more complex than just a common shifted power method. For instance, when  $\sigma = 1$  the iterates tend to follow the zigzag behavior established by Akaike [1]. In this case, it is known that for SD we have  $g_{k+1}^\top g_k = 0$  for all  $k$  and the iterates asymptotically zigzag in a 2-dimensional subspace, forcing an angle bounded away from zero between the gradient vectors and the 2 extreme eigenvectors of the matrix  $A$ . Moreover, it is also clear that in the presence of the zigzag effect the gradient vectors asymptotically tend to maintain orthogonality with all the other  $n - 2$  eigenvectors of  $A$ . Therefore, under the zigzag effect no gradient vector  $g_k$  approaches any eigenvector of  $A$ . On the positive side, once the zigzag curse is avoided, the iteration (9) resembles a shifted power method and this suggests that every so often the search direction  $g_k$  approaches some eigenvector of the matrix  $A$ . In addition, it turns out that even when the sequence of gradients does not converge to an eigenvector, it still tends to have strong components in a small number of eigenvectors, suggesting that projection processes onto subspaces of dimension larger than 1 may be useful, which we explore later in Section 3.

**Numerical setting.** In all this section and Section 3, we perform numerical tests on a quadratic functional given by a  $900 \times 900$  matrix  $A$ , obtained from the finite differences discretization of a Poisson problem on a  $30 \times 30$  grid. Throughout the paper we denote by  $\lambda_1 \leq \lambda_2 \leq \dots \leq \lambda_n$  the eigenvalues of  $A$  and  $u_1, u_2, \dots, u_n$  an associated orthonormal set of eigenvectors. We denote by  $U$  the associated unitary matrix of eigenvectors. Finally, for every method, the source term  $b$  is generated randomly and we start from a random point  $x_0 \in \mathbb{R}^n$ .

**Numerical observations.** We begin with a few illustrations of what is observed on the matrix  $A$  introduced above when using the MR and SD methods. In Figure 1, we display the Rayleigh quotients, i.e., the inverses of the steplengths  $\alpha_k^{\text{MR}}$  observed for this problem in two different cases,  $\sigma = 0.9$  and  $\sigma = 1.8$ . For  $1 < \sigma < 2$  large enough the oscillatory behavior disappears and the Rayleigh quotients seem to converge to the value  $\sigma(\lambda_1 + \lambda_n)/2$ . An example is shown in Figure 1 where  $\sigma$  takes the value 1.8. For the case  $\sigma = 0.9$  these Rayleigh quotients tend to oscillate back and forth between a high and a low value. It is remarkable that there is a ‘bias’ in the left curve: whereas the median of the eigenvalues is 4.0, here the oscillation takes place around a value significantly below this median. Visually it seems that the oscillations hover around the value 3.6 which is the product of  $\sigma$  by the median  $(\lambda_1 + \lambda_n)/2 = 4$ . This is also the value to which the Rayleigh quotients seem to converge when  $\sigma = 1.8$ . Similar observations are made for the SD method. This suggests that, when  $\sigma \in (0, 1)$ , the inverses of the steplengths span the entire spectrum, thus hitting from time to time values that are very close to an eigenvalue of  $A$ .

Next we consider the sequence of normalized residuals and examine the components of these vectors in the eigenbasis of  $A$ : we define the vectors  $(\beta_{i,k})_{i=1, \dots, n}$  given by  $U^T g_k / \|g_k\|$  (SD) or  $U^T g_k / \|g_k\|_A$  (MR) – a vector of length 900 in both cases. We plot the components of these vectors in Figure 2, for a few values of  $k$  and observe that the components of the residuals are biased toward the extremal eigenvalues. After 300 iterations, the normalized residual has a value very close to 1 in the direction  $u_1$  and a few (less than 10) components of order  $10^{-4}$  at the other end of the spectrum. After around  $k = 43$  there is not much

qualitative difference between the different figures obtained. Similarly, we plot in Figure 3 the convergence of (a few of) the normalized components  $|\beta_{i,k}|$  for different values of  $i$  along the iterations  $k$  for both the MR and SD methods. It clearly appears that, asymptotically, the intermediate modes are vanishing and the residuals are mostly supported on a few of the extremal modes.

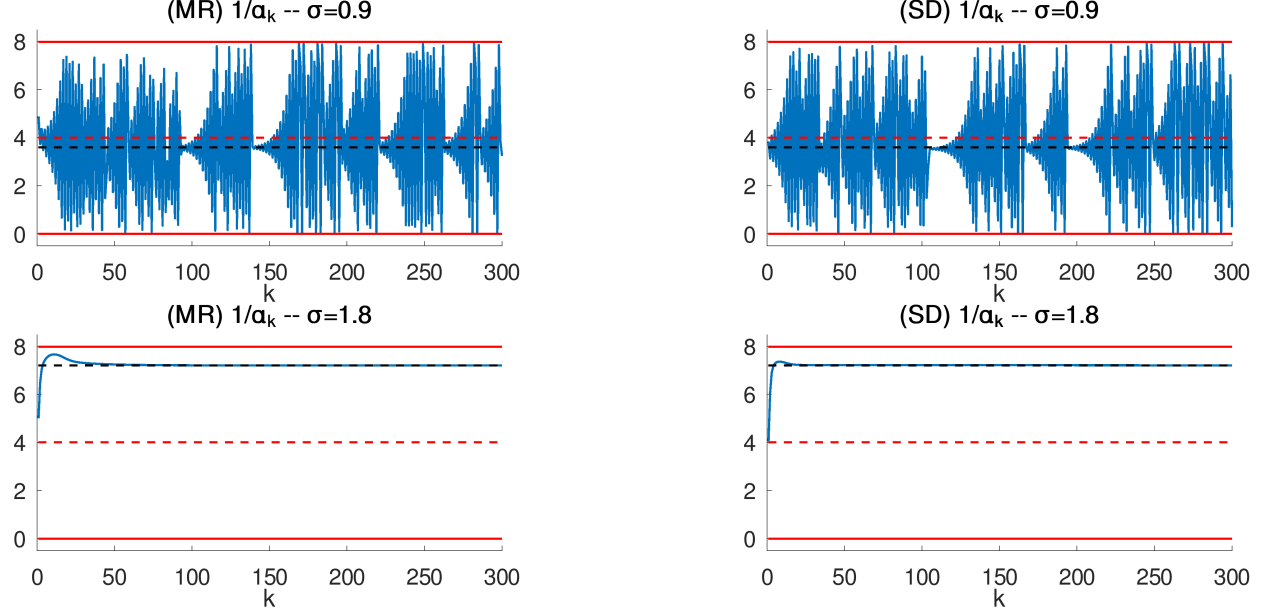


Figure 1: Sequence of Rayleigh quotients ( $1/\alpha_k$ ) with random initial gradient,  $\sigma = 0.9$  and  $\sigma = 1.8$ , for both the MR (left) and SD (right) algorithms. The top and bottom lines are the largest and smallest eigenvalues. The dashed black line is  $\sigma(\lambda_1 + \lambda_n)/2$  while the dashed red line is  $(\lambda_1 + \lambda_n)/2$ .

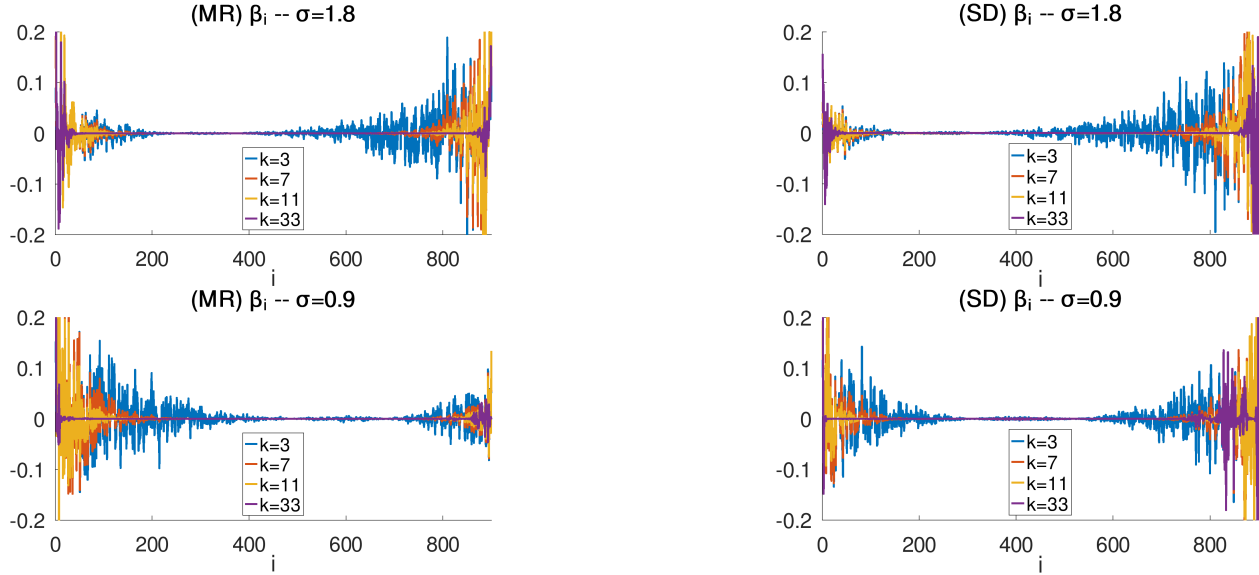


Figure 2: Components of the normalized residuals in the eigenbasis for iterations  $k = 3, 7, 11, 33$  with the MR (left) and SD (right) algorithms using  $\sigma = 0.9$  or  $\sigma = 1.8$ .

**Conclusions.** We observed numerically that, in the absence of the zigzag effect, the residuals of the MR and SD methods are asymptotically supported by a few extremal eigenmodes of the matrix  $A$ . This motivates to use this extra information in order to accelerate the convergence once the residuals are well

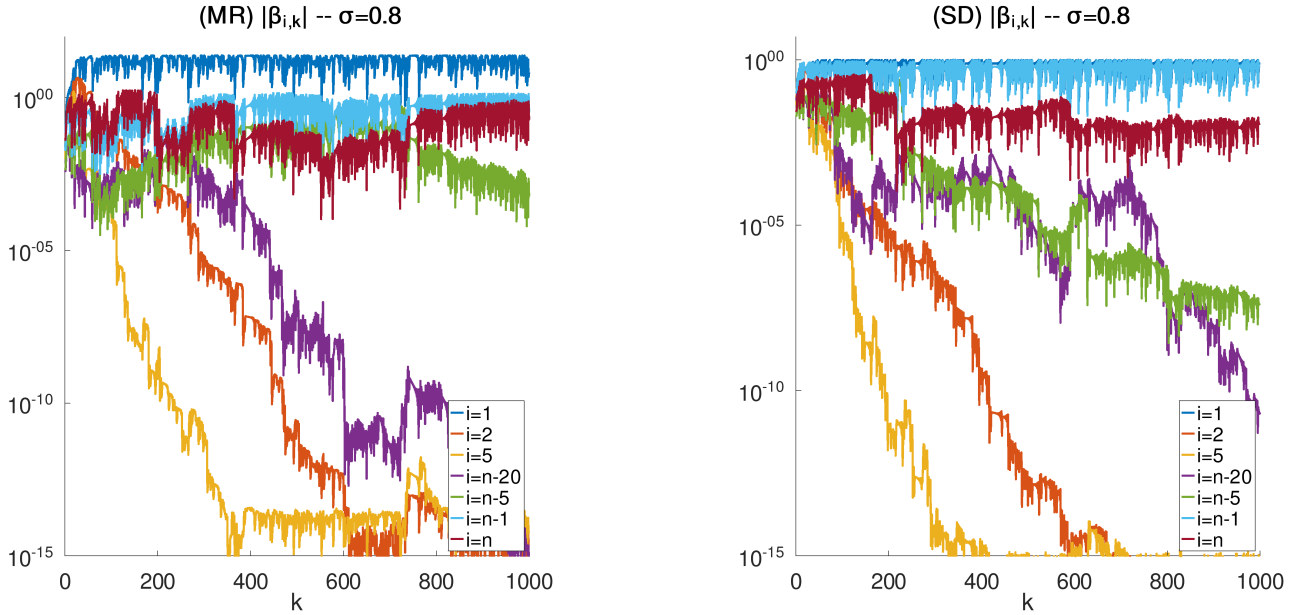


Figure 3: Convergence of  $|\beta_{i,k}|$  for different values of  $i$  and  $\sigma = 0.8$  in the case of the MR (left) or SD (right) algorithms. We used two different random initial guesses. The normalized residuals are supported by a few extremal modes (here, mostly the lowest mode  $i = 1$  and a few of the highest modes between  $i = n$  and  $i = n - 5$ ), and all the intermediate modes vanish asymptotically. Only a few modes are plotted for the sake of clarity.

approximating eigenvectors, which is the goal of the next section. Note that some of the observations we made in this section can be theoretically justified, see Section 5.

### 3 Spectral acceleration techniques

#### 3.1 Eigenvector based acceleration

##### 3.1.1 Preliminaries

Once a search direction  $g_k$  becomes a good approximation to an eigenvector of  $A$  at some iteration  $k$ , then the relaxation factor  $\sigma$  should be set to 1 in order to use the exact optimal steplength, since this optimal choice drives  $x_{k+1}$  very close to the exact solution of the minimization problem, as the following result indicates.

**Lemma 3.1** *If the iterative scheme  $x_{k+1} = x_k - \sigma \alpha_k g_k$  is used to solve (5) with  $\sigma \in (0, 2)$ ,  $\alpha_k$  obtained via (6) or (7), and at some iteration  $k \geq 1$  the gradient vector  $g_k = v$ , where  $Av = \lambda v$ , then setting  $\sigma = 1$  at iteration  $k$  results in  $x_{k+1} = x^* = A^{-1}b$ .*

**Proof.** From (6) – (7) and the fact that  $Av = \lambda v$ , we obtain that  $\alpha_k = 1/\lambda$ . Since at that iteration  $\sigma = 1$ , then  $x_{k+1} = x_k - (1/\lambda)g_k$ . Multiplying by  $A$  and subtracting  $b$  from both sides, we get:  $g_{k+1} = g_k - v = 0$ , and hence  $x_{k+1} = x^* = A^{-1}b$ . ■

Concerning the tendency to produce gradient directions that approximates an eigenvector of  $A$ , from now on we favor the use of the relaxed MR method, since it has been frequently observed that it tends to produce a next gradient direction more inclined to an eigenvector direction than the SD method; see [24] for additional details. We now present the linear convergence result of the relaxed MR method with a fixed parameter  $\sigma \in (0, 1)$  which is adapted from Theorem 8 and Lemma 11 in [18] for the specific choice  $\ell = 1/2$

and that will be required to justify the global convergence of the acceleration techniques introduced in this paper.

**Theorem 3.2** *Let  $f$  be the strictly convex function given in (5),  $\sigma \in (0, 2)$ , and  $c(\sigma)$  defined as*

$$c(\sigma) = \left(1 - \sigma(2 - \sigma) \frac{4\lambda_{\min}\lambda_{\max}}{(\lambda_{\min} + \lambda_{\max})^2}\right) < 1,$$

where  $\lambda_{\min}$  and  $\lambda_{\max}$  are the smallest and the largest eigenvalues of the Hessian matrix  $A$ , respectively. Given an initial point  $x_0 \in \mathbb{R}^n$ , for  $k \geq 0$ , let the iterates be generated by the MR method

$$x_{k+1} = x_k - \sigma\alpha_k^{MR}g_k.$$

Then

$$\|g_k\|^2 \leq c(\sigma)\|g_{k-1}\|^2 \leq \dots \leq c(\sigma)^k\|g_0\|^2. \quad (10)$$

Notice that the linear convergence result in Theorem 3.2 is based on a worst-case analysis, and in practice for  $\sigma \in (0, 1)$  the relaxed MR method requires less iterations than the slow linear rate predicted by (10). Notice also that this result, for any fixed  $\sigma \in (0, 2)$ , implies that  $\|g_k\|$  goes to zero when  $k \rightarrow \infty$ . Since  $f$  is strictly convex, by continuity it follows that the sequence  $\{x_k\}_{k \in \mathbb{N}}$  converges to  $x^* = A^{-1}b$ .

### 3.1.2 Analysis for approximate eigenvectors

We now extend the result of Lemma 3.1 to the more practical situation when the vector  $g_k = v$  is only an approximate eigenvector. Consider a step  $k$  at which we apply the iterate (2) with either (6) or (7). Either of these two steplengths is denoted by  $\alpha_k$  in what follows. If we view the current gradient direction  $g_k$  as an approximate eigenvector and we recall that  $\alpha_k^{-1}$  is the associated Rayleigh quotient, we can define the associated residual:

$$\rho_k = \frac{(A - \alpha_k^{-1} I)g_k}{\|g_k\|}. \quad (11)$$

Let us now compute the negative residual for the next iterate of the SD or MR scheme. Starting with

$$g_{k+1} = Ax_{k+1} - b = A(x_k - \alpha_k g_k) - b = g_k - \alpha_k Ag_k,$$

we see that

$$g_{k+1} = \alpha_k[\alpha_k^{-1}g_k - Ag_k] = -\alpha_k\|g_k\|\rho_k$$

We have therefore proved the following result.

**Proposition 3.3** *Assume that the iteration (2) is applied at a certain step  $k$  with either steplength (6) or (7) and let  $\rho_k$  be the residual of the vector  $g_k$  considered as an approximate eigenvector of  $A$ , as given in (11). Then the gradient of the next iterate satisfies the equality:*

$$\|g_{k+1}\| = |\alpha_k| \times \|\rho_k\| \times \|g_k\|, \quad (12)$$

in which  $\alpha_k$  stands for either  $\alpha_k^{SD}$  or  $\alpha_k^{MR}$ .

Note that we recover the case of Lemma 3.1 when  $g_k$  is an exact eigenvector since in this situation  $\rho_k = 0$  and therefore we clearly have  $g_{k+1} = 0$ . In the general situation and when  $\alpha_k$  is not large the next gradient norm is of the order of the product of the previous gradient norm and the norm of the residual norm of the same gradient considered as an approximate eigenvector. Note that the eigenvector residual norm uses a different Rayleigh quotient for each of the methods SD or MR.

Next we examine in more details the gain that can be made in one acceleration step under the above conditions. Our specific goal is to show that if the current residual  $g_k$  is a good approximate eigenvector

of  $A$ , then a projection step should result in a good reduction in the cost function, i.e., the standard Euclidean norm for MR and the  $A$ -norm of the error (or  $A^{-1}$ -norm of the residual) for SD. Since  $\sigma = 1$  for the projection step, we have

$$g_{k+1} = g_k - \alpha_k A g_k. \quad (13)$$

As the next Lemma states, the sine of the angle<sup>1</sup> between  $g_k$  and  $A g_k$  – as measured by the appropriate inner product – provides a measure of the progress made in one projection step.

**Lemma 3.4** *From one step to the next the residual norms in MR are related as follows when  $\sigma = 1$ :*

$$\frac{\|g_{k+1}\|^2}{\|g_k\|^2} = \sin^2 \angle(g_k, A g_k) \quad (14)$$

*From one step to the next the  $A^{-1}$  residual norms in SD are related as follows when  $\sigma = 1$ :*

$$\frac{\|g_{k+1}\|_{A^{-1}}^2}{\|g_k\|_{A^{-1}}^2} = \sin^2 \angle_{A^{-1}}(g_k, A g_k) \quad (15)$$

**Proof.** Inequality (14) is well-known when studying the convergence of the MR method – see for example, [20, Section 5.3.2]. The same analysis goes through to the SD case if we replace the standard inner product by the  $A^{-1}$ -inner product and norm. ■

The well-known formula (14) thus expresses the progress made in one step in terms of the angle between  $g_k$  and  $A g_k$ . Notice now that if  $g_k$  is close to an eigenvector then the angle between  $g_k$  and  $A g_k$  is small and this results in good progress from the current step to the next. We now express the fact that  $g_k$  is an approximate eigenvector by stipulating that  $A g_k = \mu_k g_k + w_k$  where  $w_k$  is a vector of small length (relative to  $g_k$ ), that is orthogonal to  $g_k$ , and  $\mu_k$  is the associated approximate eigenvalue.

**Proposition 3.5** *Let  $g_k$  be an approximate eigenvector such that*

$$A g_k = \mu_k g_k + w_k \quad (16)$$

*where  $w_k$  is orthogonal to  $g_k$  for MR, and  $A^{-1}$ -orthogonal to  $g_k$  for SD. If we assume that*

$$MR: \quad \frac{\|w_k\|}{\|g_k\|} \leq \epsilon, \quad SD: \quad \frac{\|w_k\|_{A^{-1}}}{\|g_k\|_{A^{-1}}} \leq \epsilon \quad (17)$$

*then the pair of vectors  $g_k$  and  $A g_k$  satisfy:*

$$MR: \quad \sin \angle(g_k, A g_k) \leq \frac{\epsilon}{\sqrt{\mu_k^2 + \epsilon^2}}, \quad SD: \quad \sin \angle_{A^{-1}}(g_k, A g_k) \leq \frac{\epsilon}{\sqrt{\mu_k^2 + \epsilon^2}}. \quad (18)$$

**Proof.** This proof is for the MR algorithm. An identical proof for the SD method uses  $A^{-1}$  inner products and norms<sup>2</sup>. From the assumptions  $(A g_k, g_k) = \mu_k (g_k, g_k)$  and so  $\mu_k$  is equal to the standard Rayleigh quotient of  $g_k$  with respect to  $A$ . Also  $\|A g_k\|^2 = \|\mu_k g_k + w_k\|^2 = \mu_k^2 \|g_k\|^2 + \|w_k\|^2$ . In the end, with the assumption (17) the angle  $\theta \equiv \angle(g_k, A g_k)$  is such that

$$\cos \theta = \frac{(A g_k, g_k)}{\|A g_k\| \|g_k\|} = \frac{\mu_k \|g_k\|^2}{\|g_k\| \sqrt{\mu_k^2 \|g_k\|^2 + \|w_k\|^2}} = \frac{\mu_k}{\sqrt{\mu_k^2 + (\|w_k\|/\|g_k\|)^2}} \geq \frac{\mu_k}{\sqrt{\mu_k^2 + \epsilon^2}}$$

<sup>1</sup>Recall that for an SPD matrix  $B$   $\|x\|_B^2 = (Bx, x)$  and that  $\cos_B \angle(x, y) = (Bx, y) / (\|x\|_B \|y\|_B)$ .

<sup>2</sup>Note that for SD we also assume that the relation (16) holds but that  $w_k$  is  $A^{-1}$ -orthogonal to  $g_k$  so that  $(A g_k, g_k)_{A^{-1}} = \mu_k (g_k, g_k)_{A^{-1}}$ . This means that in this case,  $\mu_k = (A g_k, g_k)_{A^{-1}} / (g_k, g_k)_{A^{-1}} = (g_k, g_k) / (A^{-1} g_k, g_k)$ .

from which we deduce

$$\sin^2 \theta \leq 1 - \frac{\mu_k^2}{\mu_k^2 + \epsilon^2} = \frac{\epsilon^2}{\mu_k^2 + \epsilon^2}.$$

Inequality (18) then follows. ■

For example a reduction by a factor of at least 2 in residual norm is obtained if  $\epsilon \leq \mu_k/\sqrt{3}$ . All these results motivates a specific treatment of the iterations for which we can detect that the residual is close to an eigenvector, in order to accelerate the convergence of the method towards the minimizer. This is the goal of what follows.

### 3.1.3 Practical application

We now discuss how to detect, without increasing the number of matrix-vector products, that  $g_k$  approaches an eigenvector of  $A$ . According to (11), the closeness can be measured by monitoring<sup>3</sup> at every iteration the normalized eigenvector-residual

$$\frac{\alpha_k}{\|g_k\|} \left\| Ag_k - \alpha_k^{-1} g_k \right\| = |\alpha_k| \|\rho_k\|. \quad (19)$$

If this eigenvector-residual is close to zero, then clearly  $g_k$  is close to an eigenvector. Moreover, if  $|\alpha_k| \|\rho_k\| < \epsilon_{\text{eig}}$  then, by Proposition 3.3, this ensures that  $\|g_{k+1}\| < \epsilon_{\text{eig}} \|g_k\|$ . Taking this remark into account, we present in Algorithm 1 our first acceleration scheme, named the ‘eigenvector acceleration scheme’.

---

#### Algorithm 1 Eigenvector Acceleration Scheme

---

```

1: Start: a given initial guess  $x_0$ ; set  $r_0 = b - Ax_0$  and  $p_0 = Ar_0$ ;
2: Choose:  $\sigma$  such that  $0 < \sigma < 1$ , and  $0 < \epsilon_{\text{eig}} < 1$ 
3: while (not converged) do
4:    $\alpha_k = \frac{p_k^\top r_k}{p_k^\top p_k}$ 
5:   if  $\frac{\alpha_k}{\|r_k\|} \left\| p_k - \alpha_k^{-1} r_k \right\| < \epsilon_{\text{eig}}$  then           ▷ Test whether  $r_k = -g_k$  is aligned with an eigendirection
6:     (recall that  $p_k = Ar_k$ ).                                     ▷ If yes, the steplength  $\alpha_k$  is optimal.
7:      $\tau_k = 1$ 
8:   else                                                       ▷ If not, use steplength  $\sigma\alpha_k$  to break the zigzag effect.
9:      $\tau_k = \sigma$ 
10:  end if
11:   $x_{k+1} = x_k + \tau_k \alpha_k r_k$ 
12:   $r_{k+1} = r_k - \tau_k \alpha_k p_k$ 
13:   $p_{k+1} = Ar_{k+1}$ 
14: end while

```

---

Our next result, obtained as a direct consequence of Theorem 3.2, establishes the convergence of the eigenvector acceleration algorithm.

**Corollary 3.6** *Let the conditions of Theorem 3.2 hold. Then the sequence  $\{x_k\}_{k \in \mathbb{N}}$  generated by the eigenvector acceleration algorithm converges to  $x^* = A^{-1}b$ .*

**Proof.** Using a fixed  $\sigma \in (0, 1)$  the eigenvector acceleration algorithm produces a subsequence  $K_1 \subset \mathbb{N}$  for which  $\tau_k = \sigma$  is used to generate the iterates. There exists a complementary subsequence  $K_2 \subset \mathbb{N}$  ( $K_1 \cup K_2 = \mathbb{N}$ ) for which  $\tau_k = 1$  is used to generate the iterates. At any iteration  $k$ , regardless of whether

---

<sup>3</sup>Note that the matrix-vector product  $Ag_k$  that appears in (19) is also required in the MR method and therefore the test does not incur significant additional computation.

$\tau_k \in (0, 1)$  or  $\tau_k = 1$ ,  $\|g_{k+1}\| < \|g_k\|$ . Therefore, the sequence  $\{\|g_k\|\}_{k \in \mathbb{N}}$  is monotonically decreasing, and since it is clearly bounded below it converges. Now, from Theorem 3.2 and the monotonicity of the entire sequence, we have that  $\{\|g_k\|\}_{k \in K_1}$  converges to zero. Consequently, the whole sequence  $\{\|g_k\|\}_{k \in \mathbb{N}}$  converges to zero, which in turn implies by continuity that the sequence  $\{x_k\}_{k \in \mathbb{N}}$  converges to  $x^* = A^{-1}b$ .

As before, the convergence result in Corollary 3.6 is based on a worst-case analysis, and in practice, thanks to what is indicated in Lemma 3.1, Lemma 3.4 and Proposition 3.5, the eigenvector acceleration algorithm requires far fewer iterations than the expected slow linear rate described in (10). We now illustrate in Figure 4 the behavior of the eigenvector-based acceleration for the matrix  $A$  introduced in Section 2. The tracked quantity in the plots is the 2-norm of the residuals  $r_k = b - Ax_k = -g_k$ . The left plot shows that (i) a significant drop is observed when the criterion from Line 5 in Algorithm 1 is activated and (ii) the convergence towards the solution is faster than with standard MR, due to break of the zigzag effect. However, on the right plot, we observe that breaking the zigzag effect with  $\tau_k = \sigma$  at every iteration (without monitoring when the residual is close to an eigenvector) produces a similar convergence history. This observation motivates the search for an alternative acceleration scheme that exploits further the search direction when it aligns with an eigenvector, as the method we introduce in the next section.

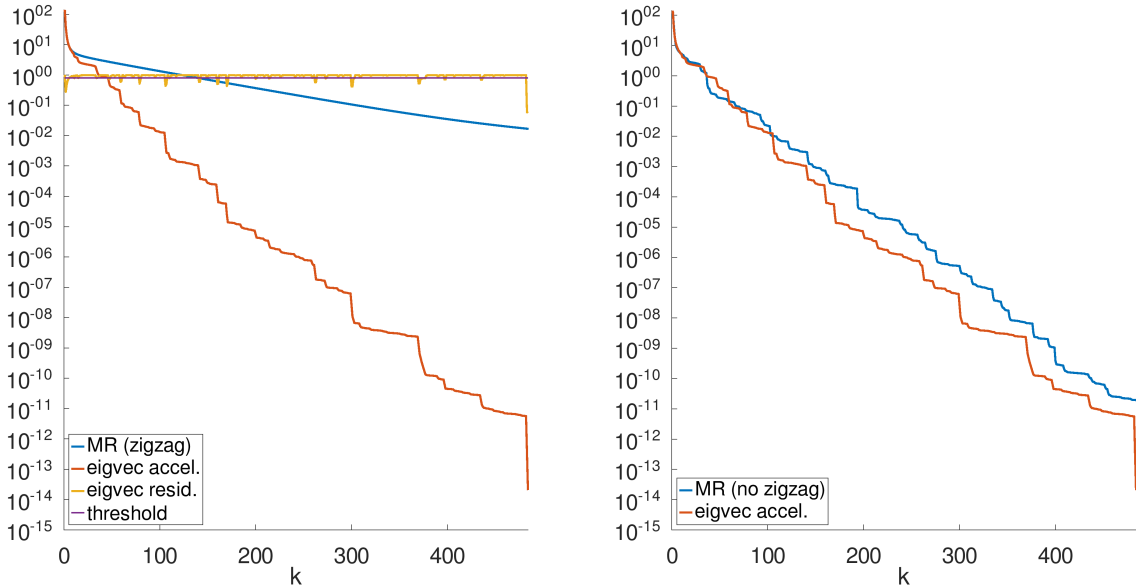


Figure 4: Eigenvector based acceleration ( $\sigma = 0.8$ ,  $\epsilon_{\text{eig}} = 0.8$ ): when the residual is close to an eigenvector (that is, the yellow line goes below the threshold), the acceleration is activated (a drop is observed on the red line). On the left, the blue line is for comparison with MR ( $\tau_k = 1$  at every iteration): it converges much slower due to the zigzag effect. On the right, the blue line is MR with  $\tau_k = \sigma \in (0, 1)$  at every iteration: it behaves similarly to the eigenvector acceleration.

### 3.2 Lanczos-based acceleration

The eigenvector acceleration idea from the previous section can be pushed further by using a few step of the Lanczos algorithm when the closeness criterion is activated. To motivate the Lanczos-based projection, we first go back to the illustration of the behavior of the residual vectors seen in Section 2, see in particular the discussion of the plots in Figure 2. There we saw that the residual vector tends to have not one large components in the eigenvectors of  $A$  but several. This means that in the transient stage it may be beneficial to project out several eigenvectors instead of just one as was done in the eigenvector acceleration

case.

We use the same activation criterion as Algorithm 1 (Line 5), after which we apply a few (say  $m \geq 1$ ) Lanczos iterations, starting from the residual vector  $r_k = -g_k$  that approximates an eigenvector, to get an orthonormal column matrix  $V_m \in \mathbb{R}^{n \times m}$  and a tridiagonal matrix  $T_m \in \mathbb{R}^{m \times m}$  such that  $T_m = V_m^T A V_m$ . Solving the least-squares problem

$$y_m = \operatorname{argmin}_{z \in \mathbb{R}^m} \|r_k - A V_m z\|^2, \quad (20)$$

we can accelerate the convergence by setting  $x_{k+1} = x_k + V_m y_m$  and  $r_{k+1} = r_k - A V_m y_m$ . Clearly, a suitable choice to start the Lanczos procedure is to take the vector  $r_k$  as its initial vector since  $r_k$  is known from the activation criterion to be a good approximation of at least one eigenvector of  $A$ . The Lanczos-based acceleration (LBA) scheme is now presented in Algorithm 2. Note that there is a structural difference between the eigenvector acceleration (Section 3.1) and the Lanczos-based acceleration that is important to highlight. The eigenvector acceleration algorithm uses two different relaxation parameters ( $\sigma \in (0, 1)$  or 1), but always uses the negative gradient direction (or residual) to generate the next iterate. Therefore, a proper use of Theorem 3.2 formally justifies its global convergence. In the Lanczos-based algorithm, there is a subsequence of iterations where the direction is no longer the negative gradient, but a modification of the gradient vector (or residual) resulting from the use of a few Lanczos iterations.

---

**Algorithm 2** Lanczos Based Acceleration (LBA)

---

```

1: Start: a given initial guess  $x_0$ ; set  $r_0 = b - Ax_0$  and  $p_0 = Ar_0$ ; a number of Lanczos steps  $m > 0$ ;
2: Choose:  $\sigma$  such that  $0 < \sigma < 1$ , and  $\epsilon_{\text{eig}} < 1$ 
3: while (not converged) do
4:    $\alpha_k = \frac{p_k^\top r_k}{p_k^\top p_k}$ 
5:   if  $\frac{\alpha_k}{\|r_k\|} \|p_k - \alpha_k^{-1} r_k\| < \epsilon_{\text{eig}}$  then            $\triangleright$  Test whether  $r_k = -g_k$  is aligned with an eigendirection
6:     (recall that  $p_k = Ar_k$ ).
7:      $V_m, T_m = \text{Lanczos}(A, r_k, m)$             $\triangleright$  If yes, perform  $m$  steps of Lanczos and update.
8:     Solve  $y_m = \operatorname{argmin}_{z \in \mathbb{R}^m} \|r_k - A V_m z\|$ 
9:      $x_{k+1} = x_k + V_m y_m$ 
10:     $r_{k+1} = r_k - A V_m y_m$ 
11:   else                                      $\triangleright$  If not, use steplength  $\sigma \alpha_k$  to break the zigzag effect.
12:      $x_{k+1} = x_k + \sigma \alpha_k r_k$ 
13:      $r_{k+1} = r_k - \sigma \alpha_k p_k$ 
14:   end if
15:    $p_k = Ar_k$ 
16: end while

```

---

**Remark 3.7** It is clear from the way in which we define the iterate  $x_{k+1} = x_k + V_m y_m$  generated by the Lanczos process, that the residual  $r_{k+1} = r_k - A V_m y_m$  satisfies  $\|r_{k+1}\| \leq \|r_k\|$ . In fact we have  $\|r_{k+1}\|^2 = \|r_k\|^2 - \|A V_m y_m\|^2$  because the optimality of  $y_m$  is equivalent to the orthogonality of  $r_{k+1}$  to the span of  $A V_m$ . This projection step is actually equivalent to a GMRES projection and the solution  $y_m$  to the minimization problem in Line 8 of Algorithm 2 can be easily computed by solving a small least-squares problem, see for instance [20, Section 6.5]. Moreover, by optimality of  $y_m$  and since the first column of  $V_m$  is proportional to the residual  $r_k = -g_k$ , it holds, after an application of the Lanczos acceleration,

$$\|g_{k+1}\|^2 \leq \|\tilde{g}_{k+1}\|^2 \leq c(\sigma) \|g_k\|^2$$

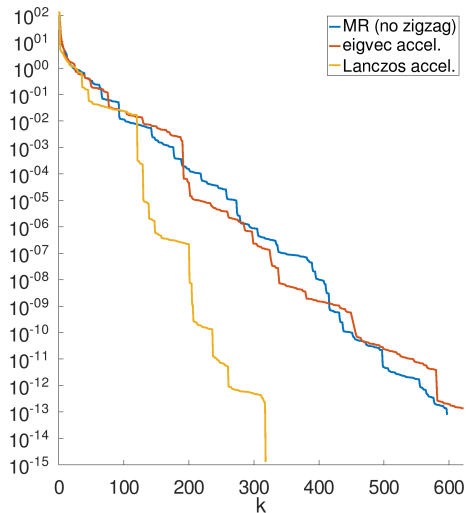
where  $\tilde{g}_{k+1}$  is the gradient after a standard MR step (no acceleration) and  $c(\sigma)$  is the constant from Theorem 3.2.

**Remark 3.8 (Case  $m = 1$ )** In the case of a single Lanczos step  $m = 1$ , the computation of  $y_m$  falls down to the minimization of  $\|r_k - zA\mathbf{r}_k\|$  over  $z \in \mathbb{R}$ , that is performing a standard MR step  $r_{k+1} = r_k - \alpha_k p_k$ . Since this is used only if the criterion on Line 5 of Algorithm 2 is triggered, this implies that LBA with  $m = 1$  is actually equivalent to the eigenvector acceleration scheme from Algorithm 1.

**Corollary 3.9** Let the conditions of Theorem 3.2 hold. Then the sequence  $\{x_k\}_{k \in \mathbb{N}}$  generated by the Lanczos-based acceleration algorithm converges to  $x^* = A^{-1}b$ .

**Proof.** Using a fixed  $\sigma \in (0, 1)$  the Lanczos-based acceleration algorithm produces a subsequence  $K_1 \subset \mathbb{N}$  for which only the relaxation parameter  $\sigma$  is used to generate the iterates. There exists a complementary subsequence  $K_2 \subset \mathbb{N}$  ( $K_1 \cup K_2 = \mathbb{N}$ ) for which the Lanczos method is activated to generate the next iterate. However, from Theorem 3.2 and Remark 3.7 we have that  $\|g_{k+1}\| \leq \sqrt{c(\sigma)}\|g_k\|$  for all  $k \in K_1$  or  $k \in K_2$ . Consequently, the whole sequence  $\{\|g_k\|\}_{k \in \mathbb{N}}$  converges to zero, which implies by continuity that  $\{x_k\}_{k \in \mathbb{N}}$  converges to  $x^* = A^{-1}b$ . ■

We now illustrate in Figure 5 the behavior of the Lanczos-based acceleration, on the same problem described in Figure 4, when compared with the eigenvector-based acceleration and also with the MR method cleared from the zigzag effect. This time, even when breaking the zigzag effect, the impact of the few Lanczos steps when the residual aligns with an eigenvector gives a significant faster convergence. Obviously, one should keep in mind that every  $m$  Lanczos steps require  $m+1$  additional matrix-vector products when triggered but the overall performance is still better (in Algorithm 2, counting only matrix-vectors products when the matrix is  $n \times n$ , there are  $m$  products in Line 7 and 1 in Line 10).



mat-vec products	
MR (no zigzag)	597
Eigenvector acceleration	622
Lanczos-based acceleration	396

Figure 5: Lanczos based acceleration ( $\sigma = 0.8$ ,  $\epsilon_{\text{eig}} = 0.8$ ): using a few steps ( $m = 5$ ) of the Lanczos algorithm makes the acceleration process more efficient, both in terms of iterations (left) and number of matrix-vector products (right). Note that, for the Lanczos-based acceleration, the number of matrix-vector products is higher than the number of iterations because every time a Lanczos projection is performed, additional matrix-vector products are used.

### 3.3 Adaptive Lanczos projection

In the previous section, a fixed number  $m$  of steps were performed in the Lanczos projection. This might not be optimal since (i) the user does not have control on the residual norm reduction performed by the projection and (ii) in the early stages of the convergence when the current iterate is far from the solution, it might not be worth performing all the Lanczos projection steps. One possibility is to use instead an adaptive strategy where, at every steps during the Lanczos algorithm, we check if the current residual is

small enough: if  $\|r_k - AV_m y_m\| \leq \text{reltol} \|r_k\|$ , then we stop the Lanczos projection at this point and can use  $y_m$  for the acceleration step as in (20), otherwise we perform an additional Lanczos step. The parameter `reltol` can then be freely chosen by the user, either as a constant smaller than 1 or a value that depends on the residual norm<sup>4</sup>. This adaptive Lanczos projection is summarized below in Algorithm 3.

---

**Algorithm 3** Adaptive Lanczos

---

```

1: Start: a given initial guess  $r$ ; the matrix  $A$ ; a relative tolerance reltol and a maximum number of
   Lanczos steps  $m$ 
2: Initialize matrices  $V_0$  and  $H_0$  as in Lanczos
3: for  $i = 1 \dots m$  do
4:   Compute  $V_i$  and  $H_i$  from  $V_{i-1}$  and  $H_{i-1}$  with one Lanczos step
5:   Solve  $y_i = \operatorname{argmin}_{z \in \mathbb{R}^i} \|r - AV_i z\|$             $\triangleright$  This is done as explained in Remark 3.10 below.
6:   if  $\|r - AV_i y_i\| \leq \text{reltol} \times \|r\|$  then
7:     break
8:   end if
9: end for

```

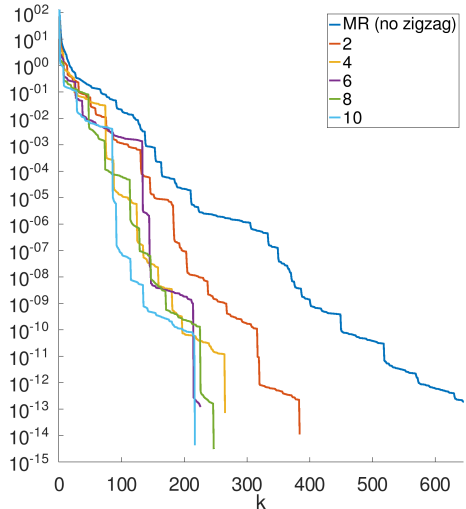
---

**Remark 3.10 (Givens rotations)** *For practical implementations of Algorithm 3, one actually only needs to update the residual until sufficient decrease is reached and compute the solution to the least-square problem. Updating the residual iteratively can be done using Givens rotations, similarly to what is done in practical implementations of GMRES, see [20, Section 6.5.3].*

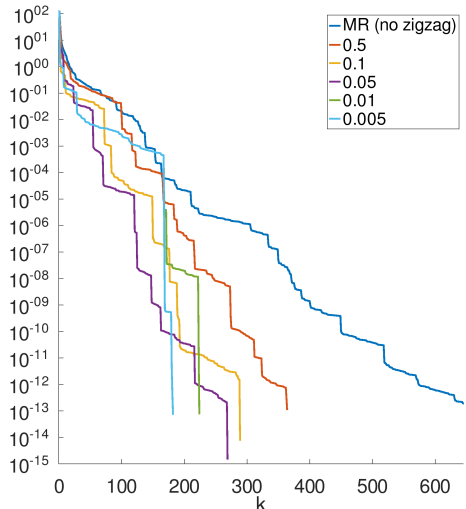
We compare this idea to having a fixed number  $m$  of Lanczos steps and we present the results in Figure 6. The conclusions are quite striking, both with a fixed number of iterations and with the adaptive version of the Lanczos algorithm. As expected, as we increase  $m$  or tighten the relative tolerance, the number of iterations decreases. Still, one has to pay attention to the total number of matrix-vector products. More precisely, regarding the LBA algorithm with a fixed number of Lanczos steps during the speed-up phase, we see that the minimum number of matrix-vectors product is achieved for  $m = 10$ . We decided not to further increase  $m$  to keep the resolution and storage cost of the least-squares problems negligible. The adaptive Lanczos with a (fixed) tight relative tolerance of  $5 \cdot 10^{-3}$  gives an algorithm that converges similarly fast, while reaching the best number of matrix-vector products. Note however that, in this case, we fixed the maximum number of Lanczos steps to  $m = 10$  and that it is reached almost everytime the projection is triggered. Finally, we ran the same experiment with an adaptive Lanczos projection where `reltol` is some power of the residual. Again, the best performance is reached for  $\text{reltol} = \|r_k\|^{1.2}$ , where very sharp acceleration are performed towards the end of the convergence (where  $m = 10$  is reached). As a conclusion, with proper choice of stopping criterion for the Lanczos projection, all these experiments yielded better convergence, both in terms of iterations and matrix-vector products, than both the standard relaxed MR algorithm and the eigenvector-based acceleration.

---

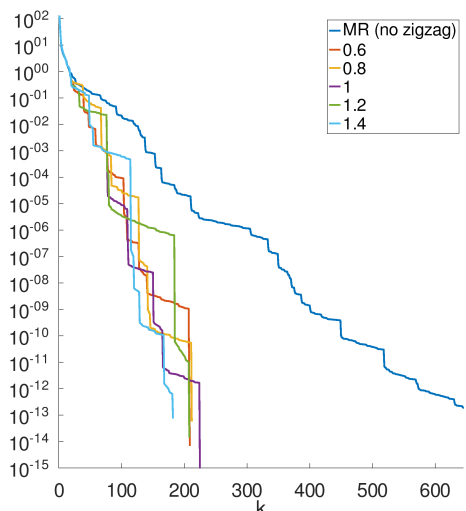
<sup>4</sup>Similarly to inexact Newton methods for instance.



m	fixed		
	iterations	matvec	calls to Lanczos
2	383	450	22
4	264	325	12
6	225	282	8
8	246	337	10
10	216	305	8



reltol	adaptive		
	iterations	matvec	calls to Lanczos
$5 \cdot 10^{-1}$	363	425	21
$10^{-1}$	288	345	10
$5 \cdot 10^{-2}$	268	361	11
$10^{-2}$	223	276	7
$5 \cdot 10^{-3}$	181	264	8



reltol	adaptive		
	iterations	matvec	calls to Lanczos
$\ r_k\ _2^{0.6}$	208	339	19
$\ r_k\ _2^{0.8}$	211	298	15
$\ r_k\ _2^1$	224	329	16
$\ r_k\ _2^{1.2}$	207	280	13
$\ r_k\ _2^{1.4}$	181	278	15

Figure 6: Lanczos-based acceleration vs MR (no zigzag, in dark blue and with reference 675 matrix-vector products) for different case. (Top) Fixed number  $m$  of Lanczos iterations when triggered. (Middle) Adaptive Lanczos projection with fixed parameter `reltol`. (Bottom) Adaptive Lanczos projection with `reltol` as some power of the residual. In the two adaptive versions, the Lanczos projections stop if  $m = 10$  is reached.

### 3.4 An analogy with algebraic multigrid methods

**Theoretical comparison** At this point we can draw an analogy between the Lanczos-based acceleration algorithm (LBA) and the basic two-grid V-cycle algebraic multigrid method (AMG) in the quadratic case:

- AMG combines approximations of the solution in spaces of different dimensions. When considering two subspaces which support the approximations of the solution, the fine space  $V_f$  is associated to a large dimensional approximation space, while the coarse space  $V_c$  is associated to a small dimensional approximation space. The basic principle of AMG consists in computing the residual  $r_f$  after some fixed iterations of a pre-smoother (typically the damped Jacobi method – DJM) in  $V_f$ , and then to restrict it to  $V_c$  as  $r_c = I_f^c r_h$ . The error  $e_c$  in  $V_c$  solves the linear system restricted to  $V_c$ :  $A_c e_c = r_c$  which is solved exactly. The next approximation of the solution is then updated by adding the extension  $e_f$  of  $e_c$  to  $V_f$  as  $e_f = I_c^f e_c$ , and an additional fixed number of iterations a post-smoother (DJM) is done. We take  $I_c^f = (I_c^c)^\top$  and a new cycle can begin. We refer to [23] for further details.
- LBA combines the approximation of the solution of the linear system on the ambient space and a correction which consists in an extension of an approximation of the current residual in a small dimensional space (obtained in the Lanczos process by few iterations of Arnoldi method). The two steps are applied alternatively (as a V-Cycle), the Lanczos acceleration is activated not after a fixed number of MR iterations but after a criterion is satisfied.

We summarize in a nutshell the parallel between the two methods in Table 1. Moreover, we presented above different versions of LBA, from the fixed number  $m$  of iterations at each Lanczos acceleration call to the various adaptive LBA with a limited  $m$  (generally  $\leq 10$ ). As an illustration of the corresponding multigrid cycle, Figure 7 (left) hereafter represents schematically an history of the MG cycle when considering the original LBA algorithm. In Figure 7 (right), we present similarly the MG cycle associated to an adaptive version of LBA where this time the dimension of the Lanczos spaces can vary. Notice that the way the coarse spaces are defined differs from a method to the other: in AMG  $V_c$  is deduced from  $V_f$  by a coarsening procedure based on matrix graph technique, associating neighbor vertices, and coupled vertices, and its dimension is fixed from the begining ; in LBA, the coarse space changes at each outer iteration, say at each application of the Lanczos process, and its dimension can vary, according to the chosen strategy (number of Lanczos iterations, adaptive or non adaptive stopping criteria).

Step	AMG	LBA
Pre-smoothing	$u := \nu$ iterations (DJM)	$u := \mu_1$ iterations (MR)
Compute residual	$r := b - Au$	$r := b - Au$
Approximate error $e_H$	$e_c := A_c^{-1} I_f^c r$	$V, H = \text{Lanczos}(r, A, m)$
Extend error to large dim space	$e_f := I_c^f e_c$	$e := Vy$
Correction	$u := u + e_f$	$u := u + Vy$
Post-smoothing	$u := \nu$ iterations (DJM)	$u := \mu_2$ iterations (MR)

Table 1: Analogy between algebraic multigrid and Lanczos-based acceleration.

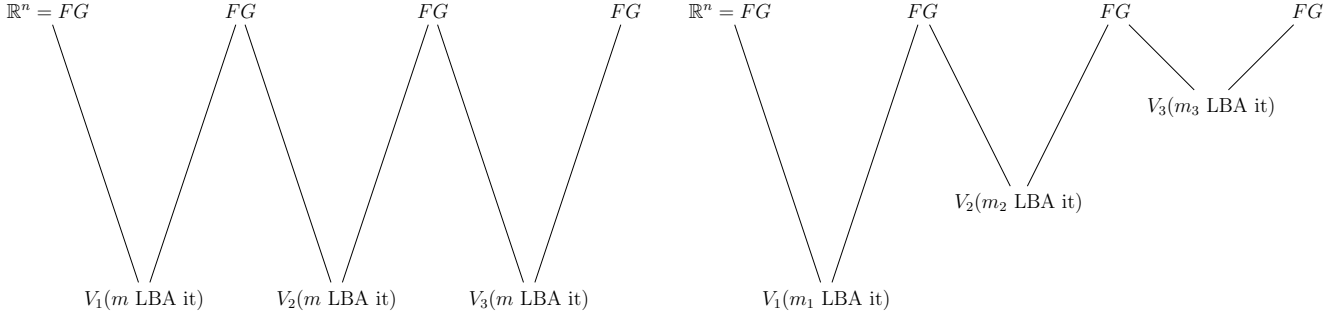


Figure 7: (Left) Multigrid-like cycle for LBA: despite the dimension of the Lanczos spaces being the same at every activation of the acceleration, the underlying spaces are built from different residuals and are thus different. (Right) Multigrid-like cycle for an adaptive LBA: this time, the dimension of the Lanczos spaces may vary at each iteration.

**Numerical comparison** In AMG, pre-smoothing and post-smoothing procedures are done by a fixed number  $\nu$  of DJM iterations while, in LBA, it is realized with a variable number  $\mu_1$  or  $\mu_2$  of MR iterations cleared from the zigzag effect. A question that can be addressed is to explore the pre-smoothing and post-smoothing procedures of AMG with the coarsening and the low dimensional solution of the system provided by the Lanczos subspace acceleration used in LBA. We give an illustration of such a combination in Figure 8 and Table 2 on the same matrix  $A$  as above (with random  $b$ ): we compare MR without the zigzag effect, LBA ( $m = 5$ ) and a two-levels method<sup>5</sup> based on Lanczos acceleration on the low dimensional space, together with a pre-smoother and post-smoother on the whole space provided by DJM iterations with a random damping coefficient ( $\beta > 0$  is a free parameter):

$$u := u + \alpha \text{diag}(A)^{-1}r \quad \text{where } \alpha \text{ follows a uniform law on } [0, \beta].$$

We observe that the acceleration criterion is still frequently activated when using a classical smoother such as DJM instead of relaxed MR and that the acceleration itself is attributable exclusively to the Lanczos subspace iterations. The values of the damping parameter  $\alpha$  also matter: an optimal (in terms of matrix-vector products) value seems to be  $\beta \approx 7.0$ . Even with such an optimal value, the LBA-DJM bi-space scheme performs only slightly better than the relaxed MR iterations (and can even fail to be monotone for  $\beta$  too large). It never outperforms LBA-MR: based on additional numerical tests, we can say that this is due to (i) the DJM producing residuals supported on much more eigenmodes than relaxed MR and (ii) the fact that relaxed MR only requires one matrix-vector product per iteration (the activation criterion can be directly computed) while DJM requires two matrix-vector products by iteration (one to evaluate the activation criterion and one to update the residuals). It is therefore crucial to couple the Lanczos subspace acceleration with a proper smoother in order to obtain significant accelerations.

LBA-DJM ( $m = 5$ )						
Value of $\beta$	0.5	1.0	5.0	7.0	10.0	15.0
iterations (matvec)	1366 (2918)	465 (1091)	214 (729)	148 (562)	196 (818)	216 (928)

Reference: MR (no zigzag): 673 (674)      LBA-MR ( $m = 5$ ): 263 (330)

Table 2: Comparison of LBA with DJM as smoother (LBA-DJM) and MR (no zigzag) or LBA with MR as smoother (LBA-MR). In parenthesis is the number of matrix-vector products, which may be larger than the actual number of iterations when Lanczos subspace iterations are used.

<sup>5</sup>The appropriate term should actually be a bi-space method rather than a multigrid method

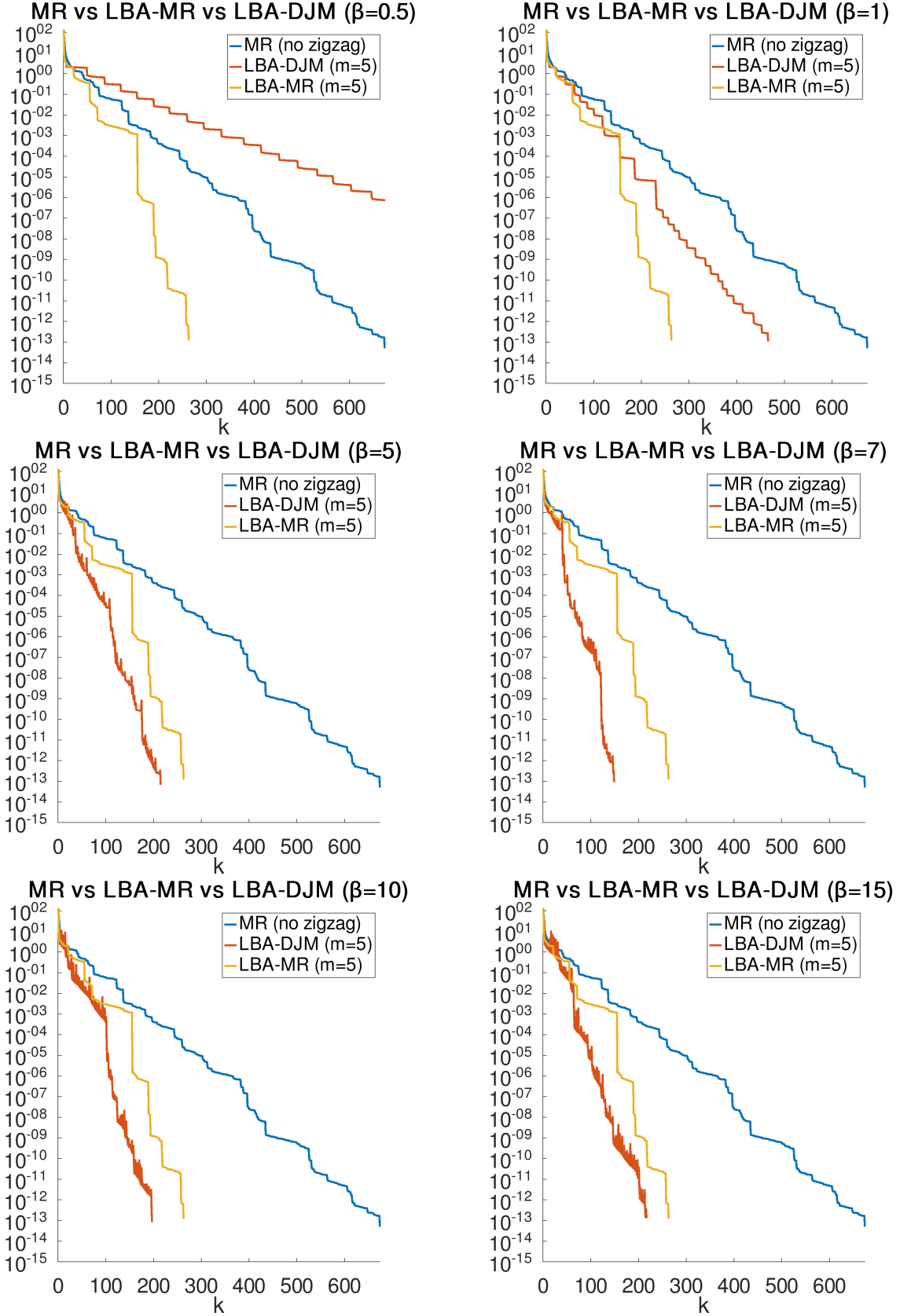


Figure 8: Comparison of the relaxed MR (no zigzag) with LBA ( $m = 5$ ) when combined with MR as smoother (LBA algorithm) and with DJM smoother, for different values of  $\beta$ .

## 4 Extension to nonquadratic convex functions

### 4.1 Incorporating line searches

In the previous section, we introduced the Lanczos based acceleration method and illustrated it on the minimization of quadratic functionals. However, for such problems, it is well known that the golden standard is the Conjugate Gradient (CG) algorithm. The CG method is optimal in the case of minimizing strictly convex quadratic functions [21], but beyond that case and without a constant Hessian, it loses its main powerful features. In the non-quadratic case, specially for convex functions, gradient-type schemes retain their simplicity and main convergence properties, which make them appealing for large-scale minimization problems. Indeed, if the cost function  $f$  is twice continuously differentiable, the eigenvector-based accelerations discussed and analyzed in Section 3 can easily be extended to non-quadratic convex functions. The residual  $r_k$  can be computed as  $-\nabla f(x_k)$  and the matrix-vector product  $Ar_k$  that appears at each iteration  $k$  of all the considered iterative schemes can be obtained, in principle, as  $-\nabla^2 f(x_k) \nabla f(x_k)$ , where  $\nabla^2 f(x_k)$  is the Hessian of  $f$  at  $x_k$ . In practice, the use of the exact Hessian of  $f$  is in most cases not feasible and not convenient in the large-scale case. Fortunately, the Hessian matrix at  $x_k$  is only required to build the matrix-vector product  $\nabla^2 f(x_k) r_k = -\nabla^2 f(x_k) g_k = -H_k g_k$ , and it can be obtained with high numerical accuracy using a finite difference approximation that only requires an additional gradient evaluation:

$$H_k g_k \approx (\nabla f(x_k + hg_k) - g_k)/h, \quad (21)$$

where  $h > 0$  is a small number. In practice, using the exact Hessian,  $\nabla^2 f(x_k)$ , or the finite difference expression in (21) produces quite similar convergence behavior for smooth convex functions.

We focus our attention on the extension of the Minimal Residual (MR) method. To the best of our knowledge, the MR method has not been extended or adapted to minimize non-quadratic convex functions. It is worth noting that the gradient-type method that has been widely extended and adapted to solve general large-scale minimization problems is the SD method [5]. These extensions of SD typically require some form of step size control or a line search.

We are thus interested in integrating the considered extensions of the MR method into a globalization technique which is as tolerant as possible, allowing the pure methods to act as freely as possible to maintain the effective accelerated behavior observed in the convex quadratic case. At the same time we expect that it affects the pure methods as little as possible, to ensure their convergence to stationary points (i.e., global minimizers in the convex case). The most suitable option for large-scale problems that satisfy these two opposing requirements is the use of undemanding line search (LS) globalization strategies.

Let us recall that, in the convex quadratic case, our schemes in Section 3 compute the steplength  $\alpha_k$  carrying out an exact line search based on closed formulas. However, the selection of an exact step-size in the general non-quadratic case is not feasible, due to the nonlinearity of  $\nabla f(x)$ . Therefore, we propose to equip the considered methods with an inexact line search. Specifically, we propose to adapt a tolerant non-monotone LS, discussed and analyzed in [17], that avoids unnecessary additional backtrackings mainly at the initial iterations, while maintaining the convergence properties, and tending to a monotonic behavior of the scheme at the final stage of the iterative process. Roughly speaking, we require at each iteration of any of the considered schemes that

$$f(x_k + \sigma \alpha_k d_k) \leq f(x_k) - \gamma (\sigma \alpha_k)^2 \|g_k\|^2 + \eta_k, \quad (22)$$

where  $\gamma$  is a small positive number,  $\eta_k > 0$  is chosen such that  $\sum_{k \in \mathbb{N}} \eta_k \leq \eta < \infty$ , and  $\sigma \alpha_k > 0$  is the steplength used to obtain the next iterate  $x_{k+1}$ . In most cases, the search direction  $d_k$  is chosen as  $d_k = -g_k$ , and  $d_k = V_m y_m$  (see Algorithm 2, step 9) when the Lanczos acceleration is activated. Notice that, in those special cases, the steplength  $\sigma \alpha_k$  is equal to 1. To extend the methods presented in Section 3 to the non-quadratic convex case, the relaxed parameter  $\sigma$  is chosen in  $(0, 1)$ , and the first trial for  $\alpha_k > 0$

is calculated using the MR formula

$$\alpha_k = \frac{g_k^\top H_k g_k}{g_k^\top H_k^2 g_k} = \frac{g_k^\top (H_k g_k)}{(H_k g_k)^\top (H_k g_k)}. \quad (23)$$

Notice that the the matrix-vector product  $H_k g_k$  is computed using (21) only once at every  $k$  and used three times in (23). We also note that the term  $\eta_k > 0$  is responsible for the sufficiently nonmonotone behavior of  $f(x_k)$ , mainly at the initial iterations of the process, and the forcing term  $-\gamma(\sigma\alpha_k)^2\|g_k\|^2$  provides the arguments for proving global convergence. In practice, to determine such a step-size  $\sigma\alpha_k$ , we use a well-known backtracking strategy, starting with  $\alpha_k$  given by (23), since this quotient exploits the local information of the objective function. Therefore, the idea is to backtrack from that step value in case it is necessary to satisfy (22).

The backtracking process is based on a safeguarded quadratic interpolation. Given  $0 < \sigma_1 < \sigma_2 < 1$  and setting  $\hat{d}_k = \sigma\alpha_k d_k$ , the safeguarding procedure acts when the minimum of the one-dimensional quadratic  $q(\cdot)$ , such that  $q(0) = f(x_k)$ ,  $q(\beta) = f(x_k + \beta\hat{d}_k)$ , and  $q'(0) = \nabla f(x_k)^\top \hat{d}_k$ , lies outside  $[\sigma_1\beta, \sigma_2\beta]$ , in which case the more conservative bisection strategy is preferred. Given a sequence  $\{\eta_k\}_{k \in \mathbb{N}}$  such that  $\eta_k > 0$  for all  $k$  and  $\sum_{k \in \mathbb{N}} \eta_k \leq \eta < \infty$ , the complete line search procedure is now described as:

---

**Algorithm 4** Line search (backtracking)

---

```

1: Input:  $\sigma \in (0, 1)$ ,  $0 < \gamma < 1$ ,  $x_k$ ,  $\alpha_k$ ,  $g_k$ ,  $d_k$ , and  $\eta_k > 0$ 
2: Set  $\hat{d}_k = \sigma\alpha_k d_k$ ,  $x_+ = x_k + \hat{d}_k$ ,  $\delta = g_k^\top \hat{d}_k$ , and  $\beta = 1$ 
3: while  $(f(x_+) > f(x_k) - \gamma(\beta\sigma\alpha_k)^2\|g_k\|^2 + \eta_k)$  do
4:    $\beta_{\text{temp}} = -\frac{1}{2}\beta^2\delta/(f(x_+) - f(x_k) - \beta\delta)$ 
5:   if  $\beta_{\text{temp}} \geq \sigma_1\beta$  and  $\beta_{\text{temp}} \leq \sigma_2\beta$  then
6:      $\beta = \beta_{\text{temp}}$ 
7:   else
8:      $\beta = \beta/2$ 
9:   end if
10:   $x_+ = x_k + \beta\hat{d}_k$ 
11: end while
12: Output:  $\sigma\alpha_k \leftarrow \beta\sigma\alpha_k$  and  $x_{k+1} \leftarrow x_+$ 

```

---

Regarding the algorithms in this section, we incorporate the LS (backtracking) described above into each of the iterative schemes considered in Section 3 to solve (1) in the convex case. To be precise, at each algorithmic step where a new iterate is computed, the candidate point passes through the LS just before the assignment to obtain a step length  $\sigma\alpha_k$  that guarantees that (22) holds. When the assignment is of type  $x_{k+1} = x_k - \tau\alpha_k g_k$ , then  $d_k = -g_k$  and the trial step length is  $\tau\alpha_k$ . When it is of type  $x_{k+1} = x_k + V y_k$  then  $d_k = V y_k$  and the trial step length is set to 1. Concerning the line search above, a few remarks are in order. We point out that, based on the smoothness of  $f$  and the presence of  $\eta_k > 0$ , it is always possible to find after a finite number of reductions of  $\beta$  a steplength  $\sigma\alpha_k > 0$  such that (22) holds. We also note that in the case of rejection of the first trial point, the next ones are computed along the same search direction. As a consequence, the gradient function is evaluated only once during the backtracking process. Finally, since the sequence  $\{x_k\}_{k \in \mathbb{N}}$  generated by any of the considered extended algorithms to solve (1) satisfies (22), it follows that for all  $k \geq 0$

$$f(x_{k+1}) \leq f(x_k) - \gamma(\sigma\alpha_k)^2\|g_k\|^2 + \eta_k.$$

Therefore, we extract the following results directly from the theoretical results in [17]:

- (Proposition 2.1 in [17]) The sequence  $\{x_k\}_{k \in \mathbb{N}}$  generated by the algorithm is contained in  $\Omega_0$ , given by  $\Omega_0 = \{x \in \mathbb{R}^n : f(x) \leq f(x_0) + \eta\}$ . Notice that  $\Omega_0$  is closed and bounded above. If  $\Omega_0$  is also bounded below then it is a compact set, which happens, for example, if  $f$  is strictly convex.
- (Theorem 2.1 in [17]) If  $\Omega_0$  is a compact set, then  $\lim_{k \rightarrow \infty} \|g_k\| = 0$ . Notice that if  $f$  is strictly convex, then by the continuity of  $\nabla f(x)$  the previous result implies that  $x_k \rightarrow x^*$ , the unique global minimizer of  $f$ .

## 4.2 Numerical experiments on strictly convex functions

Using the extended algorithms discussed above, we now illustrate the different methods and acceleration strategies on two different convex functions:

- (Strictly convex 2)  $\mathbb{R}^n \ni x \mapsto f(x) = \sum_{i=1}^n \frac{i}{10} (\exp(x_i) - x_i)$ ;
- (Logistic loss)  $\mathbb{R}^n \ni x \mapsto f(x) = \frac{\kappa}{2} \|x\|^2 + \sum_{i=1}^p \log(1 + \exp(-(x^\top z_i) y_i))$  with  $n > p$ .

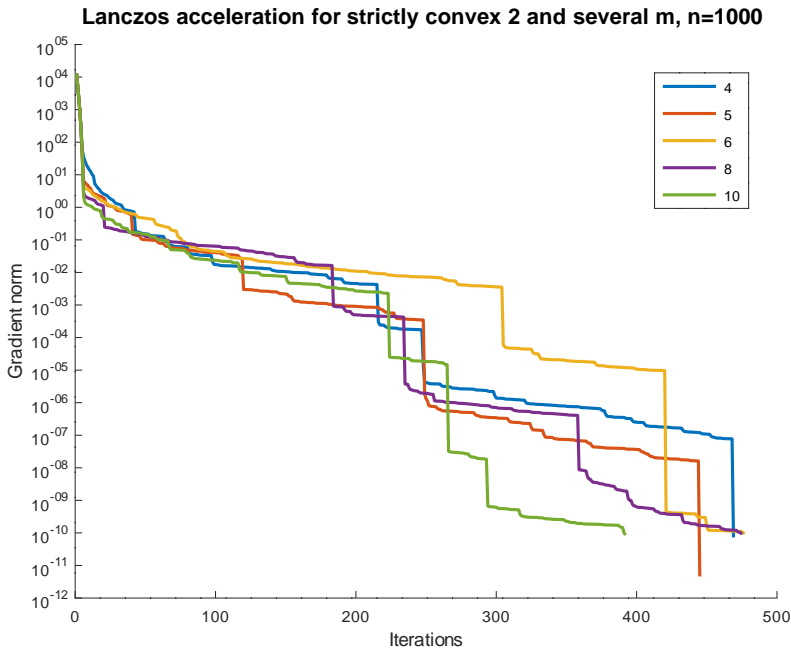
The initial guess for the strictly convex 2 function is chosen randomly in the interval  $[0, 3]$  for each component, and remains constant for all methods. For the logistic function, the initial guess is the vector of all ones, and  $z_i \in \mathbb{R}^n$  are random vectors and  $y_i$  are randomly chosen as  $\pm 1$ . All the vectors  $z_i$  and  $y_i$  remain constant for all tests, and we set  $\kappa = 0.1$ .

Concerning the approximation in (21), we set

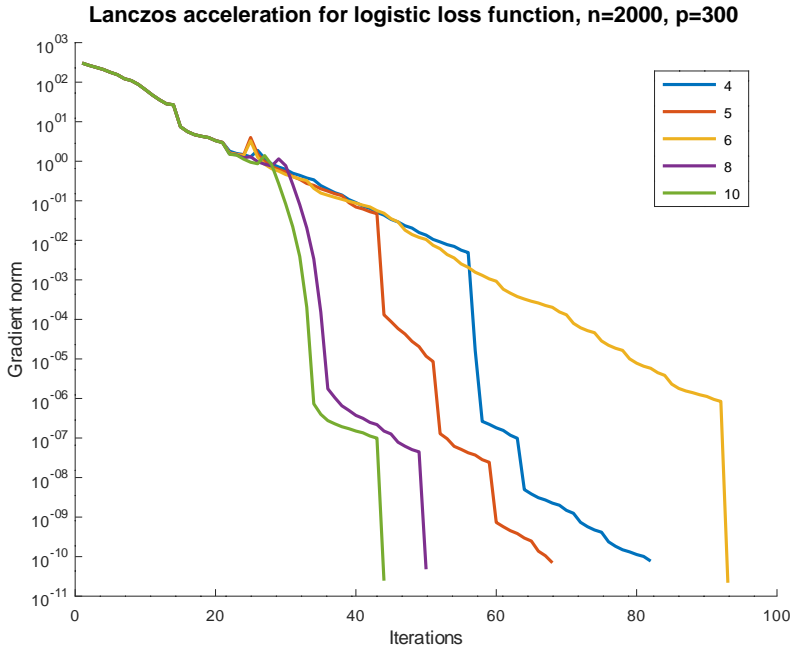
$$h = \frac{10^{-5}}{\min\{1, \max\{10^{-3}, 10^5 \|g_k\|\}\}} \in [10^{-5}, 10^{-2}].$$

Hence,  $h = 10^{-5}$  when  $\|g_k\| \geq 10^{-5}$  and  $h > 10^{-5}$  otherwise. The idea is to take  $h$  larger if  $\|g_k\|$  is too small, avoiding numerical instabilities associated with very small steps  $hg_k$ . In practice, this strategy turns out to be more effective than using a fixed  $h$ . For the line search we set  $\gamma = 10^{-4}$ , we start with  $\eta_0 = \|g_0\|$  and for  $k \geq 1$  we set  $\eta_k = \eta_0/k^{1.1}$  such that  $\sum_{k \in \mathbb{N}} \eta_k < \infty$ . In all cases, we stop the process when  $\|g_k\| \leq \text{tol}$  where  $\text{tol} = 10^{-10}$ . Finally, the relaxation parameter to avoid the zigzag effect is chosen as  $\sigma = 0.8$  and to detect an eigenvector approximation we set  $\epsilon_{\text{eig}} = 0.5$ .

In Section 3.3, we discussed two variants of adaptive Lanczos acceleration. We tested these variants on both convex functions for several dimensions and found that fixing the number of Lanczos steps ( $m$ ) consistently produced better results than the adaptive variants. Furthermore, by trying different dimensions, we observed that, on average, setting  $m = 5$  is the best option in terms of gradient evaluations, which represent the only significant computational cost in the non-quadratic case. Figure 9 shows the behavior for different values of  $m$  ( $4 \leq m \leq 10$ ) when  $f$  is the strictly convex 2 function and  $n = 1000$ , as well as when  $f$  is the logistic loss function and  $n = 2000$ ,  $p = 300$ . Based on these results, we set  $m = 5$  in our next experiments for Lanczos acceleration. Figure 10 compares the behavior of the acceleration schemes when applied to the strictly convex function 2 and  $n = 1000, 2000$ ; and Figure 11 compares the behavior of the acceleration schemes when applied to the logistic loss function when  $n = 1000$  and  $p = 200$ , and also when  $n = 2000$  and  $p = 300$ . The superiority of the Lanczos acceleration over the other accelerations in terms of gradient evaluations is clearly observed. It is worth noting that, even when backtracking is not activated, the line search strategy is essential to ensure convergence.

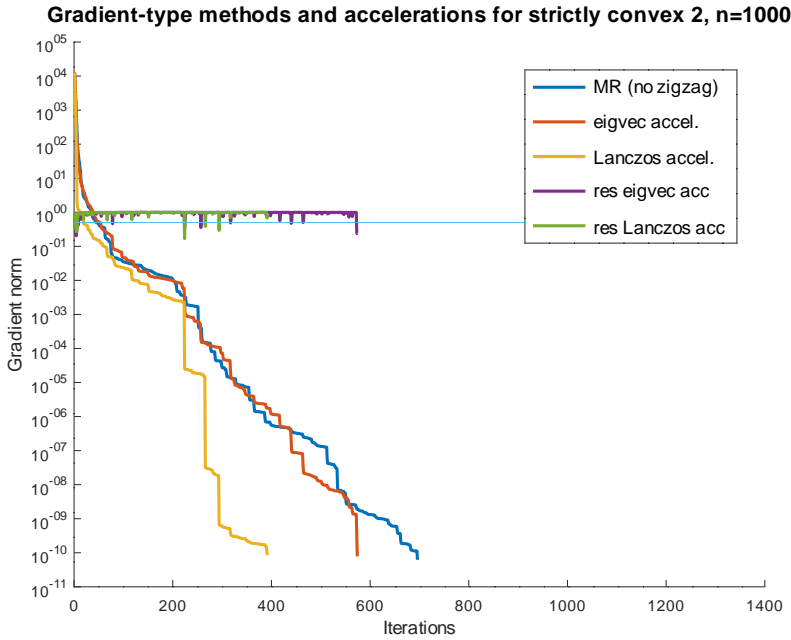


$m$	iterations	Calls to	
		Grad Eval	Lanczos
4	468	973	9
5	444	934	9
6	476	995	7
8	474	1021	9
10	391	863	8

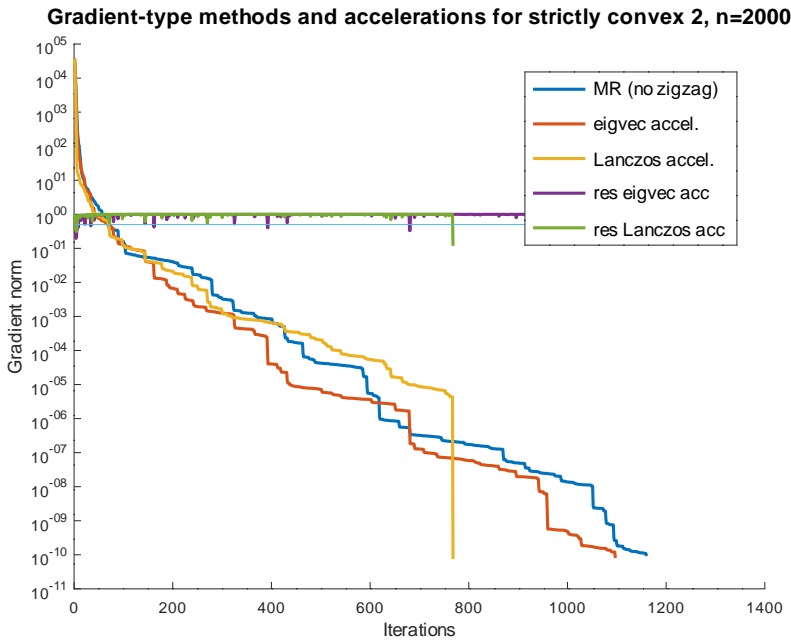


$m$	iterations	Calls to	
		Grad Eval	Lanczos
4	81	187	6
5	67	170	7
6	92	215	5
8	49	187	11
10	43	197	11

Figure 9: Lanczos-based acceleration for a variety of  $m$  Lanczos iterations when triggered. (Top) strictly convex 2 function and  $n = 1000$ . (Bottom) logistic loss function and  $n = 2000$ ,  $p = 300$ . None of the cases shown required backtrackings.



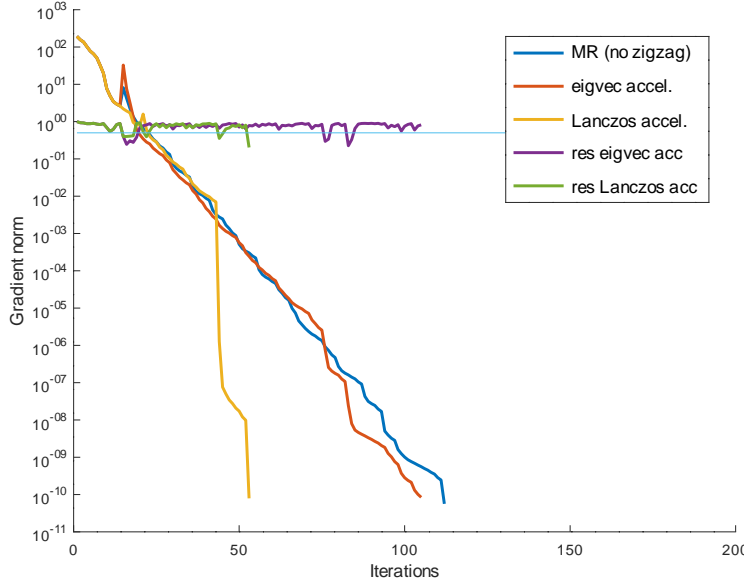
Acceleration	iterations	Grad Eval
MR (no zigzag)	695	1391
Eigenvector	573	1147
Lanczos (9)	444	934



Acceleration	iterations	Grad Eval
MR (no zigzag)	1159	2319
Eigenvector	1096	2193
Lanczos (6)	767	1565

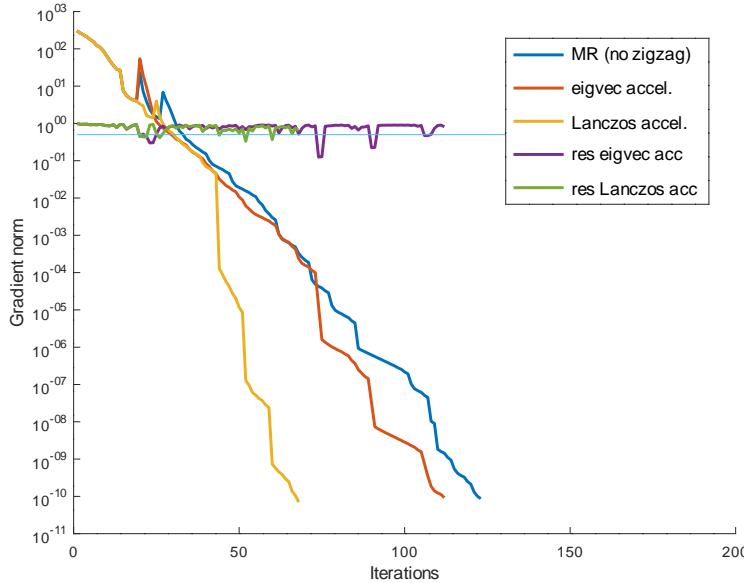
Figure 10: Performance of the acceleration schemes when applied to the strictly convex function 2. (Top)  $n = 1000$ . (Bottom)  $n = 2000$ . The number of calls to Lanczos is reported in parenthesis. None of the methods shown required backtrackings.

Gradient-type methods and accelerations, logistic loss function,  $n=1000$ ,  $p=200$



Acceleration	iterations	Grad Eval
MR (no zigzag)	111	223
Eigenvector	104	209
Lanczos (8)	52	145

Gradient-type methods and accelerations, logistic loss function,  $n=2000$ ,  $p=300$



Acceleration	iterations	Grad Eval
MR (no zigzag)	122	245
Eigenvector	111	223
Lanczos (7)	67	170

Figure 11: Performance of the acceleration schemes when applied to the logistic loss function. (Top)  $n = 1000$  and  $p = 200$ . (Bottom)  $n = 2000$  and  $p = 300$ . The number of calls to Lanczos is reported in parenthesis. None of the methods shown required backtrackings.

## 5 Detailed analysis of relaxed gradient iterations

The goal of this complementary section is to prove a number of results that justify or illustrate the behavior observed numerically in Section 2, that is the concentration of the residuals on a few extreme eigenmodes when the relaxation parameter  $\sigma$  is chosen different than 1. Again, we focus on the quadratic functional associated to a matrix  $A$ . The numerical examples illustrating this section use a  $900 \times 900$  matrix  $A$ , obtained from the finite differences discretization of a Poisson problem on a  $30 \times 30$  grid. We recall that we denote by  $\lambda_1 \leq \lambda_2 \leq \dots \leq \lambda_n$  the eigenvalues of  $A$  and  $u_1, u_2, \dots, u_n$  an associated orthonormal set of eigenvectors.

### 5.1 Preliminaries on shifted and scaled power methods

We also recall that any gradient-type method can be seen as a scaled and shifted power method for the sequence of residuals  $r_k = b - Ax_k = -g_k$  by writing

$$r_{k+1} = r_k - \sigma \alpha_k A r_k = (I - \sigma \alpha_k A) r_k = \left( \prod_{i=0}^k (I - \sigma \alpha_i A) \right) r_0. \quad (24)$$

Next, if we define, for a given nonzero vector  $v$ , the following Rayleigh quotients:

$$\mu(A, v) \equiv \frac{v^\top A v}{v^\top v}, \quad \nu(A, v) \equiv \frac{v^\top A^2 v}{v^\top A v}, \quad (25)$$

then, the steplengths (6) and (7) are nothing else than their inverses:  $\alpha_k^{\text{SD}} = \frac{1}{\mu(A, r_k)}$  and  $\alpha_k^{\text{MR}} = \frac{1}{\nu(A, r_k)}$ . They can also be seen as special cases of the generalized inverse Rayleigh quotient formula:

$$\alpha_k = \frac{r_k^\top A^{p-1} r_k}{r_k^\top A^p r_k}, \quad (26)$$

where  $p \geq 1$  is an integer number. Clearly, SD corresponds to  $p = 1$  and MR to  $p = 2$ .

We now denote the components of  $r_k$  in the eigenbasis of  $A$  by  $\beta_{1,k}, \dots, \beta_{n,k}$ . If we normalize  $r_k$  by its Euclidean norm for SD and the  $A$ -norm for MR, the  $(\beta_{i,k})_{i=1, \dots, n}$ 's will satisfy

$$(\text{SD}) : \quad \sum_{i=1}^n \beta_{i,k}^2 = 1, \quad (\text{MR}) : \quad \sum_{i=1}^n \beta_{i,k}^2 \lambda_i = 1. \quad (27)$$

Under these conditions the scalars  $(\beta_{i,k}^2)_{i=1, \dots, n}$  and  $(\lambda_i \beta_{i,k}^2)_{i=1, \dots, n}$  can be viewed as probability distributions; and the SD and MR iterations can be viewed as processes that transform these distributions: this approach is the one originally proposed by Akaike [1]. The Rayleigh quotients mentioned above can be viewed as the means of the eigenvalues under these distributions, and thus we will use the notation:

$$(\text{SD}) : \quad \bar{\lambda}_{\beta,k} = \mu(A, r_k) = \sum_{i=1}^n \beta_{i,k}^2 \lambda_i, \quad (\text{MR}) : \quad \bar{\lambda}_{\beta,k} = \nu(A, r_k) = \sum_{i=1}^n \beta_{i,k}^2 \lambda_i^2. \quad (28)$$

As convex combinations of the eigenvalues,  $\sum_{i=1}^n \beta_{i,k}^2 \lambda_i$  with  $\sum_{i=1}^n \beta_{i,k}^2 = 1$  for SD and  $\sum_{i=1}^n (\beta_{i,k}^2 \lambda_i) \lambda_i$  with  $\sum_{i=1}^n \lambda_i^2 \beta_{i,k}^2 = 1$  for MR, these weighted means will always belong to the interval  $[\lambda_1, \lambda_n]$ . A gradient step (SD or MR) thus transforms the distribution  $(\beta_{i,k})_{i=1, \dots, n}$  into a new distribution  $(\beta_{i,k+1})_{i=1, \dots, n}$  associated to a new normalized residual  $r_{k+1}$ , by applying a step of the shifted power method to the current residual  $r_k$ , where the shift changes at each step – see equation (24).

In both SD and MR, the new residual has the following components:

$$\beta_{i,k+1} = \frac{1}{s_k} \left( \frac{\bar{\lambda}_{\beta,k}}{\sigma} - \lambda_i \right) \beta_{i,k}, \quad 1 \leq i \leq n, \quad (29)$$

where  $s_k$  stands for a normalization factor, that depends on the iteration  $k$ . The magnitude of each component  $\beta_i$  is therefore ‘amplified’ by  $|\frac{\bar{\lambda}_{\beta,k}}{\sigma} - \lambda_i|/s_k$ . Since the mean  $\bar{\lambda}_{\beta,k}$  belongs to the interval  $[\lambda_1, \lambda_n]$ ,  $\bar{\lambda}_{\beta,k}/\sigma$  belongs to the interval  $[\frac{\lambda_1}{\sigma}, \frac{\lambda_n}{\sigma}]$ . The (un-normalized) amplification factors  $|\frac{\bar{\lambda}_{\beta,k}}{\sigma} - \lambda_i|$  are illustrated in Figure 12. As can be seen at every step, the highest factor is either the one associated with  $\lambda_1$  or the one associated with  $\lambda_n$ . With the assumption that  $\beta_{1,0}\beta_{n,0} \neq 0$ , it can therefore be seen that the shifted power method with the shifts equal to the inverse of generalized Rayleigh quotients will tend to produce a vector that has components only in the eigenvectors associated with these eigenvalues. However, since  $\bar{\lambda}_{\beta,k}$  depends on  $k$ , the dominating eigenvector might change from an iteration to the next. The following results help to understand this phenomenon.

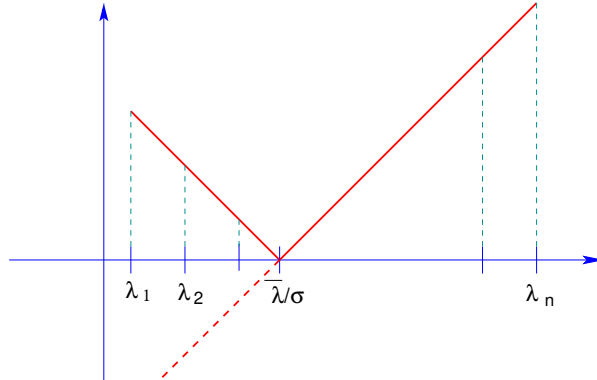


Figure 12: Amplification factors for relaxed SD / MR scheme

We define

$$\xi_k \equiv \frac{\bar{\lambda}_{\beta,k}}{\sigma} \quad (30)$$

With this notation, (29) corresponds to the shifted and scaled power method

$$r_{k+1} = \frac{1}{s_k}(\xi_k I - A)r_k. \quad (31)$$

This is a very general form, and the result shown next does not depend on how the shift  $\xi_k$  is generated but only assumes a shifted power iteration of the form (31) where  $\xi_k$  is selected from the (open) interval  $(\frac{\lambda_1}{\sigma}, \frac{\lambda_n}{\sigma})$  at each step.

**Lemma 5.1** *Let  $A \in \mathbb{R}^{n \times n}$  be a symmetric, positive definite matrix with eigenvalues  $\lambda_1 < \lambda_2 \leq \dots \leq \lambda_{n-1} < \lambda_n$  and associated eigenvectors  $(u_i)_{i=1,\dots,n}$ . Consider the following shifted and scaled power method*

$$\begin{cases} r_0 \in \mathbb{R}^n, \quad \|r_0\| = 1, \\ r_{k+1} = \frac{1}{s_k}(\xi_k I - A)r_k. \end{cases} \quad (32)$$

where  $s_k$  is a normalization factor and  $\xi_k$  is selected at each step  $k$  from the interval  $(\frac{\lambda_1}{\sigma}, \frac{\lambda_n}{\sigma})$ , with  $\sigma \in (0, 2)$ . Let  $(\beta_{i,k})_{k \in \mathbb{N}}$  be the  $i$ -th component of  $r_k$ . Assume that  $\beta_{1,0}\beta_{n,0} \neq 0$ . Then, for  $i = 1, \dots, n$

$$\begin{cases} \limsup_{k \rightarrow +\infty} \left( \prod_{j=0}^k \frac{|\xi_j - \lambda_i|}{|\xi_j - \lambda_1|} \right)^{1/k} < 1 \quad \Rightarrow \quad \lim_{k \rightarrow +\infty} \frac{|\beta_{i,k}|}{|\beta_{1,k}|} = 0 \\ \limsup_{k \rightarrow +\infty} \left( \prod_{j=0}^k \frac{|\xi_j - \lambda_i|}{|\xi_j - \lambda_n|} \right)^{1/k} < 1 \quad \Rightarrow \quad \lim_{k \rightarrow +\infty} \frac{|\beta_{i,k}|}{|\beta_{n,k}|} = 0. \end{cases} \quad (33)$$

**Proof.** Let  $i = 1, \dots, n$  and consider the first case. Applying successively  $(\xi_j I - A)$  for  $j = 0, \dots, k$  and taking the scalar product between  $r_{k+1}$  and  $u_i$ , we get for any  $k$ , after cancellation of the normalization factors,

$$\frac{|\beta_{i,k+1}|}{|\beta_{1,k+1}|} = \frac{|\beta_{i,0}| \prod_{j=0}^k |\xi_j - \lambda_i|}{|\beta_{1,0}| \prod_{j=0}^k |\xi_j - \lambda_1|} = \frac{|\beta_{i,0}|}{|\beta_{1,0}|} \prod_{j=0}^k \frac{|\xi_j - \lambda_i|}{|\xi_j - \lambda_1|}$$

Since

$$\limsup_{k \rightarrow +\infty} \left( \prod_{j=0}^k \frac{|\xi_j - \lambda_i|}{|\xi_j - \lambda_1|} \right)^{1/k} < 1 \quad \Rightarrow \quad \lim_{k \rightarrow +\infty} \prod_{j=0}^k \frac{|\xi_j - \lambda_i|}{|\xi_j - \lambda_1|} = 0,$$

we obtain the desired result. The other case is treated similarly.  $\blacksquare$

**Remark 5.2** The case where  $\beta_{1,0} = 0$  or  $\beta_{n,0} = 0$  can be easily handled:  $\lambda_1$  should be replaced by the smallest eigenvalue  $\lambda_i$  for which  $\beta_{i,0} \neq 0$  and  $\lambda_n$  by the largest eigenvalue  $\lambda_i$  for which  $\beta_{i,0} \neq 0$ . Also, the proof can be easily extended to the situation where  $\xi_k$  belongs to the closed interval  $[\lambda_1/\sigma, \lambda_n/\sigma]$  instead of being restricted to  $(\lambda_1/\sigma, \lambda_n/\sigma)$ . Indeed, if  $\xi_k = \lambda_1/\sigma$  for a given step  $k$  then  $\beta_{1,k+1} = 0$  per (29). Thus, we are in a situation similar to the one where  $\beta_{1,0} = 0$  and we can apply the same remedy: replace  $\lambda_1$  by smallest eigenvalue for which this does not happen. We can proceed similarly when  $\xi_k = \lambda_n$  for a given  $k$ .

In other words, this lemma gives a sufficient condition on the choice of the shift parameters for the normalized residuals  $i$ -th component  $(\beta_{i,k})_{k \in \mathbb{N}}$  to be negligible before the two extremal modes. In the first case in (33), the condition is equivalent to

$$\limsup_{k \rightarrow +\infty} \frac{1}{k} \sum_{j=0}^k \log \frac{|\xi_j - \lambda_i|}{|\xi_j - \lambda_1|} < 0,$$

which means that, on average,  $\frac{|\xi_j - \lambda_i|}{|\xi_j - \lambda_1|}$  is smaller than 1 but is not prevented from being larger than 1 from time to time. These considerations show that the behavior of the shifted and scaled power method depends crucially on how the  $\xi_k$ 's are chosen inside  $(\frac{\lambda_1}{\sigma}, \frac{\lambda_n}{\sigma})$ . If they are chosen as independent and identically distributed random variables, uniformly in  $(\frac{\lambda_1}{\sigma}, \frac{\lambda_n}{\sigma})$ , we can prove the following Lemma. For a more general result on random steplengths when  $\sigma = 1$ , we refer the interested reader to [16].

**Lemma 5.3** Let  $(\xi_k)_{k \in \mathbb{N}}$  be a sequence of independent random variables, uniformly distributed in  $(\frac{\lambda_1}{\sigma}, \frac{\lambda_n}{\sigma})$  for  $\sigma \in (0, 2)$ . Then, under the same setting as Lemma 5.1,

- if  $\sigma < 1$ , for any  $i \neq 1$ ,  $\limsup_{k \rightarrow +\infty} \left( \prod_{j=0}^k \frac{|\xi_j - \lambda_i|}{|\xi_j - \lambda_1|} \right)^{1/k} < 1$ . As a consequence,  $|\beta_{i,k}|$  converges to 0 for all  $i$ 's but  $i = 1$  and  $\lim_{k \rightarrow +\infty} |\beta_{1,k}| = 1$ .
- if  $\sigma > 1$ , for any  $i \neq n$ ,  $\limsup_{k \rightarrow +\infty} \left( \prod_{j=0}^k \frac{|\xi_j - \lambda_i|}{|\xi_j - \lambda_n|} \right)^{1/k} < 1$ . As a consequence,  $|\beta_{i,k}|$  converges to 0 for all  $i$ 's but  $i = n$  and  $\lim_{k \rightarrow +\infty} |\beta_{n,k}| = 1$ .
- if  $\sigma = 1$ , for any  $i \neq 1, n$ ,  $\limsup_{k \rightarrow +\infty} \left( \prod_{j=0}^k \frac{|\xi_j - \lambda_i|}{|\xi_j - \lambda_1|} \right)^{1/k} < 1$  and  $\limsup_{k \rightarrow +\infty} \left( \prod_{j=0}^k \frac{|\xi_j - \lambda_i|}{|\xi_j - \lambda_n|} \right)^{1/k} < 1$ . As a consequence,  $|\beta_{i,k}|$  converges to 0 for all  $i \neq 1, n$  and  $|\beta_{1,k}|$  and  $|\beta_{n,k}|$  cannot both converge to 0.

**Proof.** We detail the case  $\sigma < 1$  (the case  $\sigma > 1$  is treated similarly). Since  $(\xi_k)_{k \in \mathbb{N}}$  is a sequence of random variables, the idea of the proof is to rely on the equivalence

$$\limsup_{k \rightarrow +\infty} \left( \prod_{j=0}^k \frac{|\xi_j - \lambda_i|}{|\xi_j - \lambda_1|} \right)^{1/k} < 1 \Leftrightarrow \limsup_{k \rightarrow +\infty} \frac{1}{k} \sum_{j=0}^k \log \frac{|\xi_j - \lambda_i|}{|\xi_j - \lambda_1|} < 0. \quad (34)$$

By the law of large numbers, it is sufficient to compute  $\mathbb{E} \left[ \log \frac{|\xi - \lambda_i|}{|\xi - \lambda_1|} \right]$ , where  $\xi$  is a random variable uniformly distributed in  $(\frac{\lambda_1}{\sigma}, \frac{\lambda_2}{\sigma})$ , and show that it is negative for  $i \neq 1$ . To this end, let us define  $\alpha = \frac{\lambda_1}{\sigma}$  and  $\beta = \frac{\lambda_n}{\sigma}$ . Then, if  $\lambda_1 < \lambda_i < \alpha$ ,

$$\forall \xi \in [\alpha, \beta], \quad \log \frac{|\xi - \lambda_i|}{|\xi - \lambda_1|} < 0$$

and the expectation is strictly negative too. Otherwise,  $\lambda_i \geq \alpha$  and

$$\mathbb{E} \left[ \log \frac{|\xi - \lambda_i|}{|\xi - \lambda_1|} \right] = \frac{1}{\beta - \alpha} \left( \int_{\alpha}^{\beta} \log |\xi - \lambda_i| d\xi - \int_{\alpha}^{\beta} \log |\xi - \lambda_1| d\xi \right).$$

Since  $\sigma < 1$ ,  $\lambda_1 < \alpha$  and the second integral is

$$\int_{\alpha}^{\beta} \log |\xi - \lambda_1| d\xi = (\beta - \lambda_1) \log(\beta - \lambda_1) - (\alpha - \lambda_1) \log(\alpha - \lambda_1) - (\beta - \alpha).$$

As  $\lambda_i \geq \alpha$ , the first integral can be decomposed into, with the convention that  $0 \log 0 = 0$ ,

$$\begin{aligned} \int_{\alpha}^{\beta} \log |\xi - \lambda_i| d\xi &= \int_{\alpha}^{\lambda_i} \log(\lambda_i - \xi) d\xi + \int_{\lambda_i}^{\beta} \log(\xi - \lambda_i) d\xi \\ &= (\lambda_i - \alpha) \log(\lambda_i - \alpha) + (\alpha - \lambda_i) + (\beta - \lambda_i) \log(\beta - \lambda_i) - (\beta - \lambda_i) \\ &= (\beta - \lambda_i) \log(\beta - \lambda_i) + (\lambda_i - \alpha) \log(\lambda_i - \alpha) - (\beta - \alpha) \end{aligned}$$

Putting the two terms together yields

$$\mathbb{E} \left[ \log \frac{|\xi - \lambda_i|}{|\xi - \lambda_1|} \right] = \frac{1}{\beta - \alpha} \left( (\beta - \lambda_i) \log \frac{\beta - \lambda_i}{\beta - \lambda_1} + (\lambda_i - \alpha) \log \frac{\lambda_i - \alpha}{\beta - \lambda_1} + (\alpha - \lambda_1) \log \frac{\alpha - \lambda_1}{\beta - \lambda_1} \right).$$

Recall that  $\lambda_1 < \alpha \leq \lambda_i \leq \lambda_n < \beta$ . Hence, the three terms in the last sum are all negative: the expectation is therefore negative too. By (34) and Lemma 5.1,  $\frac{|\beta_{i,k}|}{|\beta_{1,k}|}$  converge to 0. Since  $r_k$  is normalized for every  $k$ , we recall that  $\sum_{j=1}^n |\beta_{j,k}|^2 = 1$ : this implies that  $|\beta_{i,k}|$  converges to 0 for  $i \neq 1$  while  $|\beta_{1,k}|$  converge to 1.

Next, if  $\sigma = 1$ , then  $\alpha = \lambda_1$ ,  $\beta = \lambda_n$ , and the calculation above shows that

$$\mathbb{E} \left[ \log \frac{|\xi - \lambda_i|}{|\xi - \lambda_1|} \right] = \frac{1}{\lambda_n - \lambda_1} \left( (\lambda_n - \lambda_i) \log \frac{\lambda_n - \lambda_i}{\lambda_n - \lambda_1} + (\lambda_i - \lambda_1) \log \frac{\lambda_i - \lambda_1}{\lambda_n - \lambda_1} \right).$$

For  $i = n$ , the expectation is thus 0 and one cannot conclude on the convergence of  $|\beta_{n,k}|$  towards 0. The calculations are similar in all the other cases. ■

The previous Lemma shows that a sufficient condition for the residual to concentrate on the extremal modes is reached when the  $\xi_k$ 's are uniformly distributed inside  $(\frac{\lambda_1}{\sigma}, \frac{\lambda_n}{\sigma})$ . This result is illustrated in Figure 13, where we track the components of the normalized residual in the eigenbasis for various  $\sigma$ . For  $\sigma < 1$ , the dominating mode is  $\beta_{1,k}$  after 100 iterations and for  $\sigma > 1$ , the dominating mode is  $\beta_{n,k}$ . For  $\sigma = 1$ , both scenarios can happen. Showing that such a condition also holds in the case of MR/SD seems a more difficult task and numerical experiments show that, when  $\xi$  is computed as in the MR or SD algorithms, such a simple convergence behavior does not seem to hold, see Figure 3.

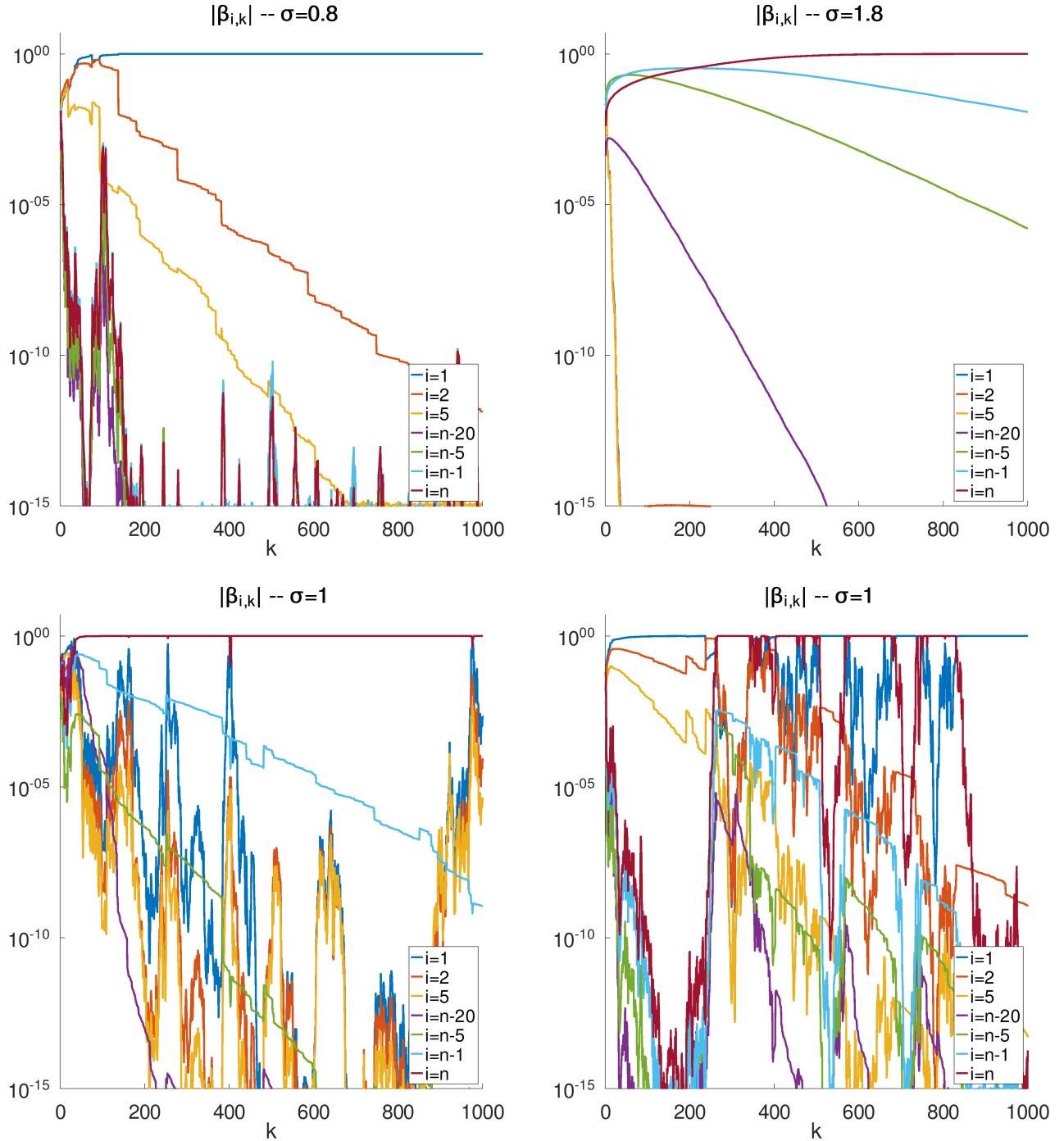


Figure 13: Convergence of  $|\beta_{i,k}|$  obtained with the shifted and scaled power method (31), for a few selected values of  $i$  and  $\sigma \in \{0.8, 1, 1.8\}$ . The  $\xi_k$ 's are chosen randomly in  $(\frac{\lambda_1}{\sigma}, \frac{\lambda_n}{\sigma})$ . When  $\sigma < 1$ , the normalized residuals are supported by the smallest mode while for  $\sigma > 1$ , the normalized residuals are supported by the largest mode (all the other modes vanish asymptotically). When  $\sigma = 1$ , one cannot conclude on the convergence of the residuals towards one of the two extremal modes, but all the other intermediate modes vanish asymptotically.

## 5.2 A simplified analysis of the relaxed SD iteration

In the previous section, we showed that, under appropriate assumptions on the shift  $(\xi_k)_{k \in \mathbb{N}}$ , the scaled and shifted power method tends to produce residuals with support on a few extreme eigenmodes. We also observed this scenario for the MR and SD algorithms without the zigzag effect in Section 2. These observations lead us to now study, without loss of generality, the situation where we have only two nonzero components  $\beta_{1,0}$  and  $\beta_{n,0}$ . First, according to (29), we recall that:

$$\beta_{1,k+1} = \frac{1}{s_k} \left( \frac{\bar{\lambda}_{\beta,k}}{\sigma} - \lambda_1 \right) \beta_{1,k}, \quad \text{and} \quad \beta_{n,k+1} = \frac{1}{s_k} \left( \frac{\bar{\lambda}_{\beta,k}}{\sigma} - \lambda_n \right) \beta_{n,k}. \quad (35)$$

To simplify notations, let us introduce

$$\gamma \equiv \frac{\lambda_1 + \lambda_n}{2}, \quad h \equiv \frac{\lambda_n - \lambda_1}{2}, \quad a_k \equiv \frac{\bar{\lambda}_{\beta,k}}{\sigma} - \gamma \quad \Rightarrow \quad \frac{\bar{\lambda}_{\beta,k}}{\sigma} - \lambda_1 = a_k + h, \quad \frac{\bar{\lambda}_{\beta,k}}{\sigma} - \lambda_n = a_k - h. \quad (36)$$

Then, (35) becomes:

$$\beta_{1,k+1} = \frac{1}{s_k} (a_k + h) \beta_{1,k}, \quad \beta_{n,k+1} = \frac{1}{s_k} (a_k - h) \beta_{n,k}. \quad (37)$$

**Lemma 5.4** *Assume that we have a 2-dimensional SD iteration with components only on the eigenvectors  $u_1$  and  $u_n$  governed by equations (37). The following then holds:*

(a) *The coefficients  $\beta_{1,k}$  and  $\beta_{n,k}$  are such that*

$$\beta_{1,k}^2 = \frac{\lambda_n - \bar{\lambda}_{\beta,k}}{\lambda_n - \lambda_1}, \quad \beta_{n,k}^2 = \frac{\bar{\lambda}_{\beta,k} - \lambda_1}{\lambda_n - \lambda_1}. \quad (38)$$

(b) *The new Rayleigh quotient  $\bar{\lambda}_{\beta,k+1}$  satisfies:*

$$\bar{\lambda}_{\beta,k+1} = \lambda_1 + \frac{1}{s_k^2} [(\lambda_n - \lambda_1)(a_k - h)^2 \beta_{n,k}^2] = \lambda_n - \frac{1}{s_k^2} [(\lambda_n - \lambda_1)(a_k + h)^2 \beta_{1,k}^2]. \quad (39)$$

(c) *The scaling factor  $s_k$  is bounded from above and below as follows:*

$$h \leq s_k \leq h + \max \left\{ \left| \frac{\lambda_n}{\sigma} - \gamma \right|, \left| \gamma - \frac{\lambda_1}{\sigma} \right| \right\}. \quad (40)$$

**Proof.**

(a) In all cases (that is for all values of  $\sigma \in (0, 2)$ ) we have the equations  $\bar{\lambda}_{\beta,k} = \beta_{1,k}^2 \lambda_1 + \beta_{n,k}^2 \lambda_n$  and  $1 = \beta_{1,k}^2 + \beta_{n,k}^2$ . From these equations we can extract  $\beta_{n,k}^2, \beta_{n,k}$  – leading to (38).

(b) The square of the normalization factor  $s_k$  is:

$$s_k^2 = (a_k + h)^2 \beta_{1,k}^2 + (a_k - h)^2 \beta_{n,k}^2. \quad (41)$$

We consider now the next Rayleigh quotient  $\bar{\lambda}_{\beta,k+1}$  to write:

$$\begin{aligned} \bar{\lambda}_{\beta,k+1} &= \frac{(a_k + h)^2 \beta_{1,k}^2 \lambda_1 + (a_k - h)^2 \beta_{n,k}^2 \lambda_n}{s_k^2} \\ &= \frac{1}{s_k^2} \left[ (a_k + h)^2 \beta_{1,k}^2 \lambda_1 + (a_k - h)^2 \beta_{n,k}^2 \lambda_1 - (a_k - h)^2 \beta_{n,k}^2 \lambda_1 + (a_k - h)^2 \beta_{n,k}^2 \lambda_n \right] \\ &= \lambda_1 + \frac{1}{s_k^2} [(\lambda_n - \lambda_1)(a_k - h)^2 \beta_{n,k}^2]. \end{aligned} \quad (42)$$

The proof of the second equality in (39) follows similarly.

(c) For the upper bound, note first that, since  $1 = \beta_{1,k}^2 + \beta_{n,k}^2$ , there exists  $\theta_1$  such that  $\beta_{1,k} = \cos \theta_1$  and  $\beta_{n,k} = \sin \theta_1$ . Then, from (41) it holds

$$\begin{aligned} s_k^2 &= (a_k^2 + 2a_k h + h^2)\beta_{1,k}^2 + (a_k^2 - 2a_k h + h^2)\beta_{n,k}^2 \\ &= a_k^2 + h^2 + 2a_k h(\beta_{1,k}^2 - \beta_{n,k}^2) \\ &= a_k^2 + h^2 + 2a_k h(\cos^2 \theta_1 - \sin^2 \theta_1) = a_k^2 + h^2 + 2a_k h \cos(2\theta_1) \\ &\leq (|a_k| + h)^2 = \left( \left| \frac{\bar{\lambda}_{\beta,k}}{\sigma} - \gamma \right| + h \right)^2. \end{aligned}$$

Thus  $s_k \leq h + |\bar{\lambda}_{\beta,k}/\sigma - \gamma|$ . The maximum is reached when  $\bar{\lambda}_{\beta,k}$  is at one of the extremes of the interval  $[\lambda_1, \lambda_n]$ . Evaluating these extreme values will yield the resulting upper bound in (40). For the lower bound it suffices to take a look at Figure 12 to see that the smallest possible value for the amplification factor  $|\bar{\lambda}_{\beta,k}/\sigma - \gamma|$  is reached when  $\bar{\lambda}_{\beta,k}/\sigma$  is in the middle of the interval  $[\lambda_1, \lambda_n]$ , i.e., when  $a_k = 0$ . For this case, (41) shows that  $s_k = h$ , which is thus the smallest possible value for  $s$ .

■

We are interested in how Rayleigh quotients evolve from one step to the next. The following result exploits the previous lemma to this end. We are also interested in the difference between  $\bar{\lambda}_{\beta,k}/\sigma$  and  $\gamma$  as this will tell how the Rayleigh quotient move relatively to the line  $\sigma\gamma$ , in order to justify the observations from Figure 1.

**Theorem 5.5** *Let the assumptions of Lemma 5.4 be satisfied. Then the following results hold.*

(a) *From one iteration to the next, the Rayleigh quotient changes as follows:*

$$\bar{\lambda}_{\beta,k+1} = \bar{\lambda}_{\beta,k} - 2 \left( \frac{\bar{\lambda}_{\beta,k}}{\sigma} - \gamma \right) \frac{(\lambda_n - \bar{\lambda}_{\beta,k})(\bar{\lambda}_{\beta,k} - \lambda_1)}{s_k^2}. \quad (43)$$

*As a result,  $\bar{\lambda}_{\beta,k+1}$  will decrease from  $\bar{\lambda}_{\beta,k}$  if  $\bar{\lambda}_{\beta,k} > \sigma\gamma$  and will increase when  $\bar{\lambda}_{\beta,k} < \sigma\gamma$ .*

(b) *In addition, (43) can be rewritten as:*

$$\left( \frac{\bar{\lambda}_{\beta,k+1}}{\sigma} - \gamma \right) = \left( \frac{\bar{\lambda}_{\beta,k}}{\sigma} - \gamma \right) \left[ 1 - 2 \frac{(\lambda_n - \bar{\lambda}_{\beta,k})(\bar{\lambda}_{\beta,k} - \lambda_1)}{\sigma s_k^2} \right] \quad (44)$$

*which means that  $\bar{\lambda}_{\beta,k+1}$  will change sides relative to the biased median  $\sigma\gamma$  whenever*

$$\sigma s_k^2 < 2(\lambda_n - \bar{\lambda}_{\beta,k})(\bar{\lambda}_{\beta,k} - \lambda_1) \quad (45)$$

*or equivalently, when*

$$\frac{\left( \frac{\bar{\lambda}_{\beta,k}}{\sigma} - \lambda_1 \right)^2}{\left( \bar{\lambda}_{\beta,k} - \lambda_1 \right)} + \frac{\left( \lambda_n - \frac{\bar{\lambda}_{\beta,k}}{\sigma} \right)^2}{\left( \lambda_n - \bar{\lambda}_{\beta,k} \right)} < \frac{2(\lambda_n - \lambda_1)}{\sigma}. \quad (46)$$

*In particular, when  $\sigma = 1$  this inequality will always be satisfied which implies that the Rayleigh quotient will oscillate around  $\gamma$  in this case.*

(c) *When  $\sigma \geq 2\lambda_n/(\lambda_1 + \lambda_n)$  then the sequence of Rayleigh quotients  $\bar{\lambda}_{\beta,k}$  converges. In any situation when  $\bar{\lambda}_{\beta,k}$  converges its limit is either  $\lambda_1$ , or  $\lambda_n$  or  $\sigma\gamma$ .*

**Proof.**

(a) We start from the two relations (39). Multiplying them respectively by  $\beta_{1,k}^2, \beta_{n,k}^2$  and adding them yields

$$\bar{\lambda}_{\beta,k+1} = \bar{\lambda}_{\beta,k} + \frac{(\lambda_n - \lambda_1)\beta_{1,k}^2\beta_{n,k}^2}{s_k^2} \left[ (a_k - h)^2 - (a_k + h)^2 \right] = \bar{\lambda}_{\beta,k} - 4a_k h \frac{(\lambda_n - \lambda_1)\beta_{1,k}^2\beta_{n,k}^2}{s_k^2}. \quad (47)$$

Replacing  $h$  and  $a_k$  with their definitions in (36) and using (38), we obtain

$$\bar{\lambda}_{\beta,k+1} = \bar{\lambda}_{\beta,k} - 2 \left( \frac{\bar{\lambda}_{\beta,k}}{\sigma} - \gamma \right) \frac{(\lambda_n - \lambda_1)^2 \beta_{1,k}^2 \beta_{n,k}^2}{s_k^2} = \bar{\lambda}_{\beta,k} - 2 \left( \frac{\bar{\lambda}_{\beta,k}}{\sigma} - \gamma \right) \frac{(\lambda_n - \bar{\lambda}_{\beta,k})(\bar{\lambda}_{\beta,k} - \lambda_1)}{s_k^2} \quad (48)$$

(b) Let us go back to (47) which gives

$$\bar{\lambda}_{\beta,k+1} = \bar{\lambda}_{\beta,k} - 2a_k \frac{(\lambda_n - \lambda_1)^2 \beta_{1,k}^2 \beta_{n,k}^2}{s_k^2} \quad (49)$$

Dividing by  $\sigma$  and subtracting  $\gamma$  we finally obtain

$$\frac{\bar{\lambda}_{\beta,k+1}}{\sigma} - \gamma = \frac{\bar{\lambda}_{\beta,k}}{\sigma} - \gamma - 2a_k \frac{(\lambda_n - \lambda_1)^2 \beta_{1,k}^2 \beta_{n,k}^2}{\sigma s_k^2} = \left( \frac{\bar{\lambda}_{\beta,k}}{\sigma} - \gamma \right) \left[ 1 - 2 \frac{(\lambda_n - \lambda_1)^2 \beta_{1,k}^2 \beta_{n,k}^2}{\sigma s_k^2} \right] \quad (50)$$

which can be written as

$$a_{k+1} = a_k \left( 1 - 2 \frac{1}{\sigma t_k} \right) \quad \text{with} \quad t \equiv \frac{s_k^2}{d^2 \beta_{1,k}^2 \beta_{n,k}^2} \quad \text{and} \quad d \equiv \lambda_n - \lambda_1. \quad (51)$$

According to (38) the term  $d^2 \beta_{1,k}^2 \beta_{n,k}^2$  equals  $(\lambda_n - \bar{\lambda}_{\beta,k})(\bar{\lambda}_{\beta,k} - \lambda_1)$ . In order for  $\bar{\lambda}_{\beta,k}$  to change sides with respect to  $\sigma\gamma$ , we need to have  $1 - 2/(\sigma t) < 0$ , i.e.,  $\sigma t < 2$ . This happens when (45) is satisfied. Also from (41) :

$$t = \frac{(a_k + h)^2}{d^2 \beta_{n,k}^2} + \frac{(a_k - h)^2}{d^2 \beta_{1,k}^2} = \frac{1}{d} \left[ \frac{\left( \frac{\bar{\lambda}_{\beta,k}}{\sigma} - \lambda_1 \right)^2}{(\bar{\lambda}_{\beta,k} - \lambda_1)} + \frac{\left( \lambda_n - \frac{\bar{\lambda}_{\beta,k}}{\sigma} \right)^2}{(\lambda_n - \bar{\lambda}_{\beta,k})} \right], \quad (52)$$

from which (46) follows. Finally, when  $\sigma = 1$  the left hand side of (46) evaluates to  $(\bar{\lambda}_{\beta,k} - \lambda_1) + (\lambda_n - \bar{\lambda}_{\beta,k}) = \lambda_n - \lambda_1$ : (46) is always satisfied when  $\sigma = 1$ .

(c) Since  $\bar{\lambda}_{\beta,k} \leq \lambda_n$ , when  $\sigma \geq 2\lambda_n/(\lambda_1 + \lambda_n)$  we have  $\bar{\lambda}_{\beta,k}/\sigma \leq \gamma$ . Thus, according to (43), the Rayleigh quotients  $(\bar{\lambda}_{\beta,k})_{k \in \mathbb{N}}$  form an increasing sequence which is bounded from above by  $\lambda_n$  and it will therefore converge. We now need to determine their limit, assuming just that the sequence converges.

Assume the limit is neither  $\lambda_1$  nor  $\lambda_n$ . Then, equation (38) from Lemma 5.4 shows that (both)  $\cos^2 \theta_1 = \beta_{n,k}^2$  and  $\sin^2 \theta_1 = \beta_{1,k}^2$  will converge to a positive value. Since  $s_k$  is bounded from above independently of the iteration  $k$ , per (40), equation (43) implies the desired result that  $|\bar{\lambda}_{\beta,k}/\sigma - \gamma|$  converges to zero.

■

This theorem explains partly the behavior of the relaxed SD iteration. If at a given step the Rayleigh quotient  $\bar{\lambda}_{\beta,k}$  is above the biased median, i.e. if  $\bar{\lambda}_{\beta,k}/\sigma - \gamma > 0$ , then (43) indicates that in the next step the new Rayleigh quotient decreases from its current value. In the opposite situation, it will increase.

We now explore inequality (46) a little further. It can be shown that the left-hand side is of the form  $f(\bar{\lambda}_{\beta,k})$  where

$$f(t) = \frac{\lambda_n - \lambda_1}{\sigma} \left( 2 - \frac{1}{\sigma} \right) + \left( \frac{1}{\sigma} - 1 \right)^2 \left[ \frac{\lambda_1^2}{t - \lambda_1} + \frac{\lambda_n^2}{\lambda_n - t} \right]. \quad (53)$$

An illustration is shown in Figure 14. The curve decreases from the left pole to a minimum achieved at the harmonic mean  $2/(1/\lambda_1 + 1/\lambda_n)$  and increases to infinity at its right pole. The left pole is extremely

sharp: for  $t = \lambda_1 + 10^{-6}$  the value is still only 13.15923.. In most of the interval the inequality will be satisfied which means that the Rayleigh quotient will *generally* oscillate around the biased median. If  $\bar{\lambda}_{\beta,k}$  happens to fall above the dashed line (say close to the right pole), then according to part (a) of the theorem, it will decrease in the next step. It will then either converge or cross the line and start oscillating again. From our experience,  $\bar{\lambda}_{\beta,k}$  converges only when  $\sigma$  is large enough (close to 2).

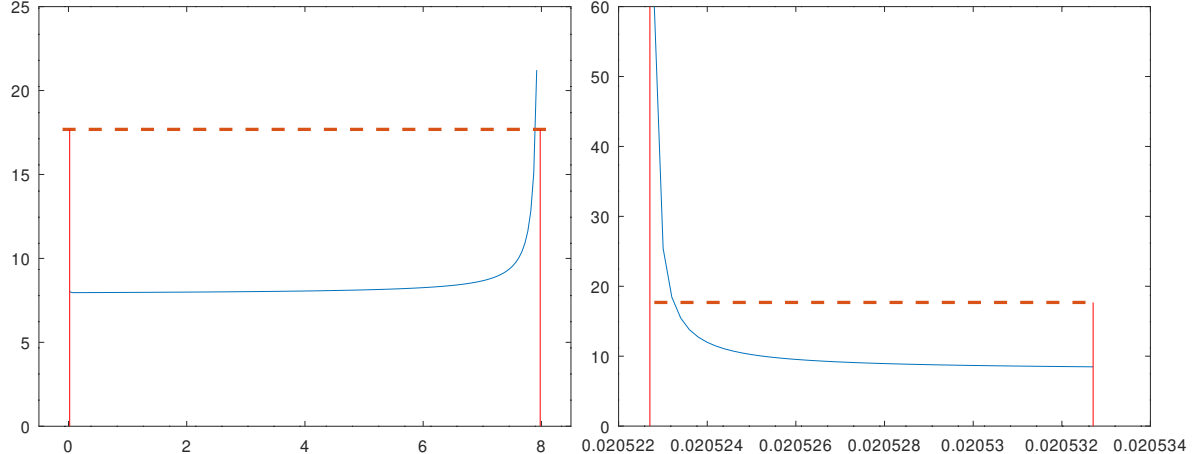


Figure 14: Illustration of inequality (46) with  $\sigma = 0.9$ . The solid line is the left-hand side of (46) as a function of  $\bar{\lambda}_{\beta,k}$ . The dashed one is the constant of the right-hand side. The pole on the left side is not visible because the curve is extremely sharp around it (right). – The right figure shows a zoom in interval  $[\lambda_1 + 10^{-7}, \lambda_1 + 10^{-5}]$

The case  $\sigma = 1$  has received extensive coverage in the literature. In this case, the scalar  $t$  defined in (52) in the proof of the theorem is equal to one. Therefore (51) becomes  $a_{k+1} = -a_k$  or  $\left(\frac{\bar{\lambda}_{\beta,k+1}}{\sigma} - \gamma\right) = -\left(\frac{\bar{\lambda}_{\beta,k}}{\sigma} - \gamma\right)$ . Thus,  $\bar{\lambda}_{\beta,k}$  will *equi-oscillate* exactly around  $\sigma\gamma$ . One special case when  $\bar{\lambda}_{\beta,k}$  converges is when  $\bar{\lambda}_{\beta,k}/\sigma$  is always below the median  $\gamma$  which takes place in the particular situation stated in part (c) of the theorem. It may be possible to establish that  $\bar{\lambda}_{\beta,k}$  converges when  $\sigma$  is  $< \lambda_n/(\lambda_n + \lambda_1)$  but larger than a certain  $\sigma_*$ . Although we cannot prove this, our experience does show that a large  $\sigma$  often leads to convergence of the Rayleigh Quotients. See Figure 1 (right) for an example showing a situation when  $\bar{\lambda}_{\beta,k}$  converges.

In summary, the relaxed SD iteration leads to a situation where the residual lies in a one or two-dimensional space. When  $\sigma < 1$ , the Rayleigh quotients will tend to oscillate around  $\sigma\gamma$  and for this reason the gradient will tend to converge (in direction) to the smallest eigenvector. Although this analysis was restricted to the SD scheme, the same behavior is observed in practice for MR and it is therefore likely that similar results might be proved. Finally, note that there are other scenarios depending on the value of  $\sigma$  but what matters practically for the acceleration schemes developed in this paper is that the gradient will be close to an eigenvector or a linear combination of a small number of eigenvectors.

## Acknowledgments and fundings

All the authors are grateful to Université de Picardie Jules Verne for financial support of Yousef Saad's stay in Amiens and to LAMFA (UPJV and CNRS, UMR 7352) for financial support of Marcos Raydan's stay in Amiens, both in March 2025.

The third author is funded by national funds through the FCT – Fundação para a Ciência e a Tecnologia, I.P., under the scope of the projects UID/00297/2025 (<https://doi.org/10.54499/UID/00297/2025>) and

UID/PRR/00297/2025 (<https://doi.org/10.54499/UID/PRR/00297/2025>) (Center for Mathematics and Applications). The work of the fourth author was supported by NSF grant: DMS-2513117.

## Data availability

All the simulations have been performed with a GNU Octave implementation of the algorithms and can be downloaded at

<https://plmlab.math.cnrs.fr/gkemlin/lba-paper>

## References

- [1] H. AKAIKE, *On a successive transformation of probability distribution and its application to the analysis of the optimum gradient method*, Annals of the Institute of Statistical Mathematics, 11 (1959), pp. 1–16.
- [2] N. ANDREI, *Modern numerical nonlinear optimization*, vol. 195, Springer, 2022.
- [3] S. BELLAVIA, T. BIANCONCINI, N. KREJIĆ, AND B. MORINI, *Subsampled first-order optimization methods with applications in imaging*, in *Handbook of Mathematical Models and Algorithms in Computer Vision and Imaging: Mathematical Imaging and Vision*, Springer, 2023, pp. 61–95.
- [4] S. BELLAVIA, N. KREJIĆ, B. MORINI, AND S. REBEGOLDI, *A stochastic first-order trust-region method with inexact restoration for finite-sum minimization*, Computational Optimization and Applications, 84 (2023), pp. 53–84.
- [5] D. P. BERTSEKAS, *Nonlinear Programming*, 2nd ed., Athena Scientific optimization and computation series, Athena Scientific, Belmont, MA, 1999.
- [6] L. BOTTOU, F. CURTIS, AND J. NOCEDAL, *Optimization methods for large-scale machine learning*, SIAM Review, 60 (2018), pp. 223–311.
- [7] A. L. CAUCHY, *Méthode générale pour la résolution des systèmes d'équations simultanées*, Comp. Rend. Academ. Sci., 25 (1847), pp. 536–538.
- [8] Y.-H. DAI AND Y.-X. YUAN, *Alternate minimization gradient method*, IMA Journal of numerical analysis, 23 (2003), pp. 377–393.
- [9] R. DE ASMUNDIS, D. DI SERAFINO, W. W. HAGER, G. TORALDO, AND H. ZHANG, *An efficient gradient method using the yuan steplength*, Computational Optimization and Applications, 59 (2014), pp. 541–563.
- [10] R. DE ASMUNDIS, D. DI SERAFINO, F. RICCIO, AND G. TORALDO, *On spectral properties of steepest descent methods*, IMA Journal of Numerical Analysis, 33 (2013), pp. 1416–1435.
- [11] D. DI SERAFINO, V. RUGGIERO, G. TORALDO, AND L. ZANNI, *On the steplength selection in gradient methods for unconstrained optimization*, Applied Mathematics and Computation, 318 (2018), pp. 176–195.
- [12] G. FRASSOLDATI, L. ZANNI, AND G. ZANGHIRATI, *New adaptive stepsize selections in gradient methods*, Journal of Industrial & Management Optimization, 4 (2008), pp. 299–312.
- [13] C. C. GONZAGA AND R. M. SCHNEIDER, *On the steepest descent algorithm for quadratic functions*, Computational Optimization and Applications, 63 (2016), pp. 523–542.

- [14] L. GRIPPO AND M. SCIANDRONE, *Introduction to methods for nonlinear optimization*, vol. 152, Springer Nature, 2023.
- [15] Y. HUANG, Y.-H. DAI, X.-W. LIU, AND H. ZHANG, *On the asymptotic convergence and acceleration of gradient methods*, Journal of Scientific Computing, 90 (2022), pp. 1–29.
- [16] Z. KALOUSEK, *Steepest Descent Method with Random Step Lengths*, Foundations of Computational Mathematics, 17 (2017), pp. 359–422.
- [17] W. LA CRUZ AND G. NOGUERA, *Hybrid spectral gradient method for the unconstrained minimization problem*, Journal of Global Optimization, 44 (2009), pp. 193–212.
- [18] L. MACDONALD, R. MURRAY, AND R. TAPPENDEN, *On a family of relaxed gradient descent methods for strictly convex quadratic minimization*, Computational Optimization and Applications, 91 (2025), pp. 173–200.
- [19] M. RAYDAN AND B. F. SVAITER, *Relaxed steepest descent and cauchy-barzilai-borwein method*, Computational Optimization and Applications, 21 (2002), pp. 155–167.
- [20] Y. SAAD, *Iterative Methods for Sparse Linear Systems, 2nd edition*, SIAM, Philadelphia, PA, 2003.
- [21] Y. SAAD AND H. A. VAN DER VORST, *Iterative solution of linear systems in the 20th century*, J. Comp. Appl. Math, 123 (2000), pp. 1–33. Numerical analysis 2000, Vol. III. Linear algebra.
- [22] K. VAN DEN DOEL AND U. ASCHER, *The chaotic nature of faster gradient descent methods*, Journal of Scientific Computing, 51 (2012), pp. 560–581.
- [23] J. XU AND Z. LUDMIL, *Algebraic multigrid methods*, Acta Numerica, (2017), pp. 591–721.
- [24] B. ZHOU, L. GAO, AND Y.-H. DAI, *Gradient methods with adaptive step-sizes*, Computational optimization and applications, 35 (2006), pp. 69–86.
- [25] Q. ZOU AND F. MAGOULÈS, *Delayed gradient methods for symmetric and positive definite linear systems*, SIAM Review, 64 (2022), pp. 517–553.